



## Introduction

The long shutdown at CERN is now coming to an end and it is therefore a good moment to review what changes it has brought. The year 2013 has been declared as *the injector year*. In the case of ISOLDE it has been marked by an extensive upgrade of the facility. In the target area new target-handling robots, target-dismantling hot cell, and access system have been installed. The problem with the GPS extraction electrode has been identified and repaired. The ISCOOL has been realigned and re-cabled to avoid sparking. At the infrastructure level the target building is being enlarged, to host the MEDICIS project, which will use the protons traversing the ISOLDE target for production and separation of isotopes tailored for medical studies (see more details in the contribution of Th. Stora). The RILIS cabin has been extended and a remote-control system of the lasers is under development. It will be most probably implemented for the run of 2014.

After many negotiations we had enough funds to demolish bldgs. 115, 507, and 601 located behind the ISOLDE hall at the Jura side, and to plan a unified building, bldg. 508, that will be ready in May 2014. On the bottom floor, building 508 will host larger laser and solid-state laboratories, a new detector laboratory and the previously existing workshop. Outside the controlled area, on the first floor, the ISOLDE control room will be located together with the data acquisition rooms, a kitchen and a visitor room overlooking the ISOLDE hall. The latter has been motivated by the change in classification of the ISOLDE hall, from the point of view of radio-protection, that will at the start-up pass from supervised to basic controlled area. The visitor room will enable ISOLDE to accommodate the large amount

of external visits from students to dignitaries from the present and future CERN member states.

The HIE-ISOLDE infrastructure works are progressing well, the new compressor and cold box buildings, bldg. 198 and 199 respectively, are slowly being filled with different equipment. Inside the ISOLDE hall, the new linac tunnel, the ventilation in the hall extension and many new cable trays have been put in place. The exiting mezzanine has been rebuilt to accommodate the power supplies for the linac.

The great interest of our community in the new physics that will be accessible with higher energy beams at HIE-ISOLDE is reflected by the fact that 27 experiments with a total of 627 shifts have already been approved, for physics from day one. The plan for HIE-ISOLDE phase I (see the contribution of Y. Kadi) has not changed; the commissioning of the superconducting linac is expected to start in June 2015 and the first physics experiments in the autumn of the same year.

This "calm" year for the users has been extremely fruitful for the analysis of data and publications of results. The number of publications in 2013 was close to one hundred among them three papers in Nature (Nature 497, p. 199-204 and 498, p. 346-349) and Nature Communications (43, p. 141-146) and several in Phys. Rev. Letts and Phys. Letts. At the same time a great effort has been made regarding outreach with several contributions that appeared in the CERN Bulletin (21/28 January and 29 July 2013), CERN Courier (Volume 53, Jan-Feb (n. 1), April (n. 3) and June (n.5) 2013), PH-Newsletters and in Nuclear physics News (Vol. 23, April-June 2013, a feature article about masses, and the potentiality of CRIS is described in facilities and methods). The outcome of these joint efforts from the users and the in-house

group has been an increase of visibility of ISOLDE at CERN and elsewhere that highly benefits our community and the HIE-ISOLDE project. Details of the results obtained from different ISOLDE experiments are described in this newsletter and many were discussed and presented at the ISOLDE workshop held the 25-27 November 2013 <https://indico.cern.ch/event/263071/>. This was followed by a two day workshop <https://indico.cern.ch/event/255042/> where the advances in the design study part of the HIE-ISOLDE project concerning increase in purity, beam intensity and quality were presented. This design study will be described in a report that will be submitted to CERN in October 2014.

A great effort has been dedicated during this shutdown period to make the ISOLDE website (<http://isolde.web.cern.ch>) a site of communication for the users and a tool to diffuse our activities. The new layout was developed and the content of the previous website transferred thanks to Jenny Weterings. The website will have the updated information of the new conditions to access the experimental hall as soon as it is available.

To enhance the connection of the users to the facility a series of courses were organized <http://isolde.web.cern.ch/isolde-schools-and-courses>. The first one entitled "Statistical Tools for Nuclear Experiments" was given by Dr K. Riisager from 18-21 of March and the second course was given by Prof. R. Casten from the 23-26 of July with the title 'ISOLDE nuclear physics summer lectures series'. The third course was entitled 'Shell model course for non-practitioners' and it was lectured by E. Caurier, G. Martinez-Pinedo, F. Nowacki, A. Poves, K. Sieja. A fourth course will be offered from the 22-25 of April 2014 entitled 'ISOLDE Nuclear Reactions and Nuclear Structure'. The course will address the different information that can be

obtained by studying reactions at the energies relevant for HIE-ISOLDE concerning both the nuclear structure and the reaction process. The lecturers will be W. Catford, A. Di Pietro and A. Moro. Practical exercises including optical model and DWBA calculations using FRESCO are foreseen as well as the use of TWOFNR code for transfer (d,p) reactions. The response to this initiative by the different groups was excellent to the point that we were obliged to limit the attendance when practical work was offered.

The implementation of the TSR, a 55 metre circumference storage ring from Heidelberg, was well received by CERN management. The TSR will be connected to the post-accelerated beams of HIE-ISOLDE phase II and will allow beams to be cooled and stored for decay, in-ring reaction experiments as well as being extracted to external setups. The beam properties, such as transverse emittance and momentum spread, will each be reduced at least one order of magnitude compared to HIE-ISOLDE linac values, and for lighter ions the effective intensity will be significantly increased owing to the recirculation of the beam. A study focussing on the technical integration of the ring into the CERN accelerator infrastructure was carried out by E. Piselli, E. Siesling and F. Wenander. The report was presented in August 2013, and provided information about the costs and required manpower. CERN has recognised the unique scientific opportunity offered by installing the TSR at the HIE-ISOLDE facility, and the case for the TSR has been presented to and endorsed by the Scientific Policy Committee. The Research Board has given outline approval for the TSR, although the timeline has not yet been defined. Several groups have manifested their commitment to develop instrumentation for the TSR and different working groups have

been created after the fruitful workshop that took place in February 2014.

During 2013 no ENSAR funds have been used. The project will finish in August 2014 although a prolongation until the end of the year is expected. Meanwhile the preparation for the ENSAR-2 application is ongoing. The incorporation of new facilities into the transnational access including ECT\* is being contemplated.

I would like to finish by reminding you that it is now 50 years since the approval of ISOLDE in December 1964. ISOLDE was connected to the synchro-cyclotron, SC, the first accelerator at CERN and received the first beams in 1967. The SC has become a historical device for the European Physical Society and it will be opened to the public in a ceremony on the 19th of June 2014. With very few interruptions, ISOLDE has remained as the pioneer ISOL-installation both at the level of designing new devices and production of frontier Physics. **We are just counting the weeks until the restart!**

*Maria J.G. Borge*

## Information for Users:

### Registration and access to ISOLDE

The recent break in online experiments at ISOLDE gives me a good opportunity to remind everybody of the procedures to enter CERN and ISOLDE.

### Registering as a CERN user

The Spokesperson of the scheduled experiment should check who will participate in it and whether their institute is part of the proposal (which can be verified via the [Greybook](#)). If it is not, please contact Jenny at the ISOLDE User Support Office and enquire how to add the

institute to the experiment. Otherwise the person will not be able to register.

The rules for registering as a CERN user changed at the beginning of 2012, therefore all of you requiring a new registration or registration prolongation should check the User-Office website and ISOLDE website to get the latest info.

### Access to ISOLDE

The rules for accessing the ISOLDE hall will change on July 1st this year, when the hall will change from RP supervised to RP simple controlled area. **This means that access will be registered in the personal dosimeter not the CERN card and temporary dosimeters will not be accepted to enter the facility.** All permanent dosimeters should be returned to the dosimetry service and there will be flexibility in getting them back.

To get the permanent dosimeter and to get access to ISOLDE users will have to: (i) present a form signed by their institute, which replaces the medical certificate, (ii) follow an ISOLDE on-line RP course, and (iii) follow a 2-hour practical training session. Therefore, if you want to get access to ISOLDE before the weekend, you will have to come at the latest on Thursday evening, in order to register and follow the course during Friday working hours. At the same time, the new building behind ISOLDE (bldg. 508) will host several DAQ rooms located outside the RP-area, where those without the dosimeters will be able to follow their experiments. We will inform you when we get more detailed information on the courses and the RP form.

### When at ISOLDE

Until the end of 2014 due to HIE-ISOLDE infrastructure installation the ISOLDE hall will be divided into two parts. The access for ISOLDE physicists will be possible only from the Jura side, and with access

recorded in the dosimeter. Access to the ISOLDE hall extension will require separate access rights. Moving of equipment (e.g. LN<sub>2</sub> dewars) through that part of the hall should be coordinated with Erwin Siesling and will require safety shoes and helmet. For the low-energy area we are discussing the possibility of waiving the requirement for safety shoes and helmets.

### **CERN Hostel booking**

Following our 2012 initiative to have 10 hostel rooms booked for people on shift, we have been able to increase to 20 rooms in 2014 for the period of August 1 until December 19. As in 2012, the booking requests should be grouped by the spokespersons and communicated to Jenny. Please use this group booking only when you can't book the room in the regular way.

### **Other practical info**

Other recent practical information (alternative accommodation options, accident insurance, free bike and car rental, etc.) can be found on our [website](#) and in the Newsletters 2012 and 2013.

*Magdalena Kowalska*

## Status of the HIE-ISOLDE Project.

The High Intensity and Energy (HIE)-ISOLDE project aims at several important upgrades of the present ISOLDE radioactive beam facility at CERN. The main focus lies in the energy upgrade of the post-accelerated radionuclide beams from 3 MeV/u up to 10 MeV/u through the addition of superconducting cavities. This will open the possibility of many new types of experiments including transfer reactions throughout the nuclear chart. Phase 1 of this upgrade involves the design, construction, installation and commissioning of two high- $\beta$  cryomodules downstream of REX-ISOLDE, the existing post-accelerator. Each cryomodule houses five high- $\beta$  superconducting cavities and one superconducting solenoid. Prototypes of the Nb-sputtered Quarter Wave Resonators (QWRs) cavities for the new superconducting linear accelerator have been manufactured and are undergoing RF cold tests.

The project also aims at improving the target and front-end part of ISOLDE to fully benefit from potential upgrades of the existing CERN proton injectors e.g LINAC4 and upgrade in energy of the PS Booster (see contribution of R. Catherall).

### **Integration and Layout:**

The new HIE-ISOLDE superconducting linear accelerator will require a major increase of equipment to the existing facility's infrastructure. Two new surface buildings have been constructed in order to house the helium compressor station and the helium refrigerator cold box (Fig.1).

Ground breaking started at the end of summer 2011 with the preparation of the site and the construction of a new lock to allow access of personnel and material to the experimental hall. The construction

works were completed by the third quarter of 2012 after which the installation of the electrical systems and main services have taken over.



*Fig.1: New HIE-ISOLDE buildings*

The cryogenic station installation (Figs.2&3) started in the first quarter of 2014. The LHe liquefier will be installed in a separate light construction building as close as possible to the linac in order to minimize the length of the LHe distribution line. This will enable an easier and more stable operation of the cryogenic system.

The cryogenic system to be supplied includes one cryogenic transfer line, which will link the cold box and the different interconnecting ("jumper") boxes feeding from the top, the six cryomodules of the new SC linac.

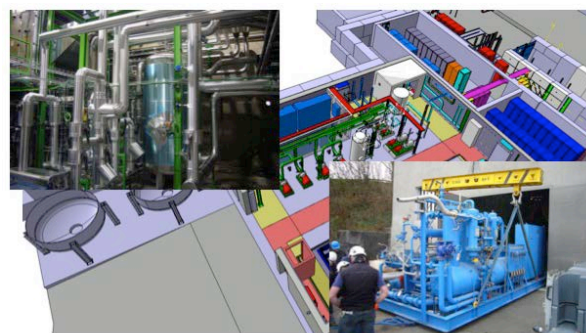


*Fig.2: Compressor skit/frame arrived in B198. Compressors sent off for refurbishment*

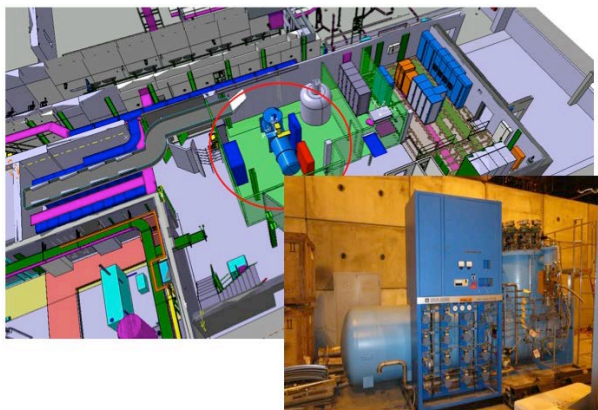


**Fig.3:** ex-ALEPH, presently at LHC point 4. Necessary material for refurbishment has arrived at the contractor (LINDE). Before sending to the company a leak test will be performed at CERN

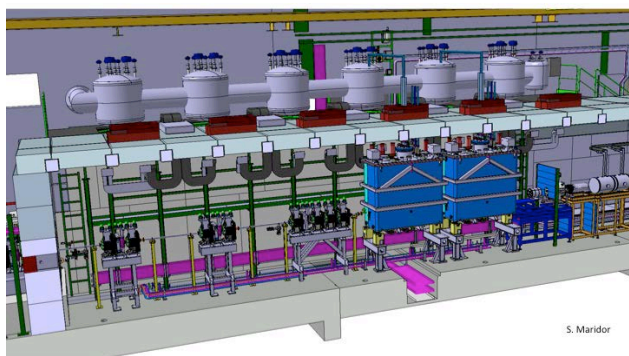


**Fig.4:** Cryo Cold Line & Jumper Boxes installation: Sept 2014 – Jan 2015 (construction Line, Jumper Boxes & Dewar (2000L) ongoing at CRIOTEC).

Cryo Module 1 installation: April – June 2015,  
Cryo Module 2 installation: Shutdown 2015/16:  
Jan – March 2016

A new high-energy beam transfer line (HEBT) will bring the beam into the existing extension of the ISOLDE experimental hall [4].

In Phase 1 only the first two high-beta cryomodules will be installed in the tunnel. Downstream from the existing REX linac, they will boost the radioactive ion beam energy to 5.5MeV per nucleon and deliver the beam to two experimental stations via the first stage of the HEBT (Fig.6).

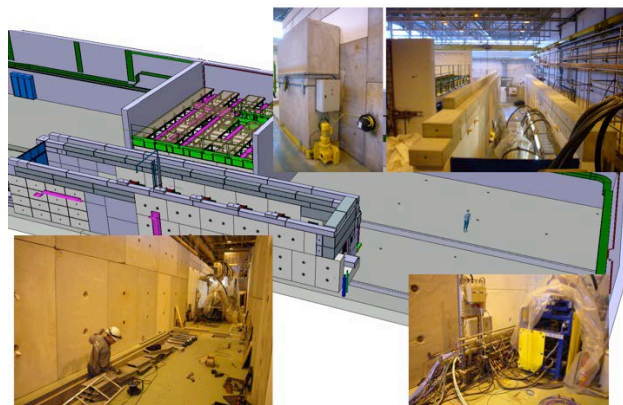


**Fig.5:** Shielding tunnel walls and door in place. Preparing for infrastructure inside the tunnel: Inside metal structure – starts as of end April (1wk); Jumper boxes platform installation as of beginning May (3 wks); Vacuum and water infrastructure – May/June; Cable trays and cabling May/July; Flexwell RF cables Sept/Oct; Linac/HEBT supports in tunnel in place by August.

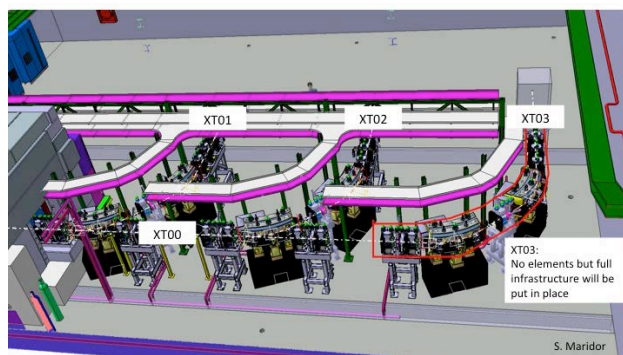


**Fig.6:** Layout of the High Energy Transfer lines in the ISOLDE experimental hall.

The MINIBALL segmented Ge array and T-REX experimental setups already operational at REX will be used intensively when the first beams are delivered in 2015. An open beam line will also be available for traveling experiments. In this context, an active-target experiment for resonant scattering and transfer reactions is also under consideration.

The HEBT will be extended in a second stage of the installation foreseen during 2017/18 to accommodate a third

experimental station and to allow for the connection to a storage ring (TSR) [6].



**Fig.7:** First stage of the HIE Linac and beamlines. HEBT carrying structure for cable trays and infrastructure being installed; HEBT cable trays and cabling installation as of April; water cooling and vacuum infrastructure as of May; HEBT elements will arrive as of September. Prioritized installation: XT00/01 to be ready by mid-Feb 2015, XT02 by mid- April 2015.

**High Beta cavities:**

The development of the superconducting cavities started in 2008 and focussed on the high-beta cavity design, which will be installed first. The cavities are based on the Nb sputtered on Cu technology pioneered at LNL-Legnaro. They are specified to reach a nominal accelerating field of 6 MV/m on axis

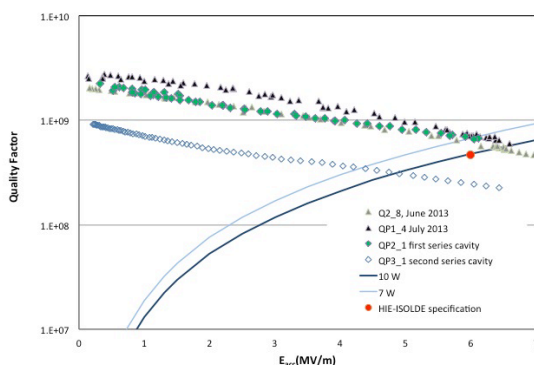


**Fig.8:** RF Test results (last two prototypes and first two series).

over an active length of 300 mm. A Q-value of  $5 \cdot 10^8$  is necessary to reach this field with a power dissipation of 7 W. In recent years much effort has been put into the design of a coating facility and the optimisation of the coating process. The latest cavities went up to 6 MV/m at 7 W, 30% above the design goal. Further details can be found in [7]. QP3 (2<sup>nd</sup> series cavity) did not reach nominal performance. The precise cause is not clear but could be associated with the following:

- Copper from a different manufacturer than the one chosen for the industry production, different machinability was noticed
- Probably some part of the RF surface was contaminated

The decision was taken to strip and coat the cavity again. So far the overall success rate for sputtering is 75% and we hope to increase this performance.

Company delay on prototypes (4 months)  
Pre machining of series advancing  
Expected delivery of #1 and #2 end of April

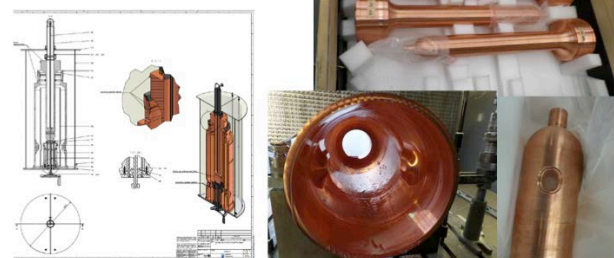


**Fig.9:** Cavity production in industry.

The fundamental power coupler and tuning systems were designed and prototypes are available [11], [12]. However, a continuing effort is being put in reviewing and improving the existing designs, both on economic and on technical grounds.

The first model of fundamental power coupler showed some mechanical problems after several thermal cycles between warm and operational temperatures. At the end of 2011 a redesign of this element was

launched and the first prototype was successfully tested in March 2012.

The new design is based on a stainless steel external body to minimize the thermal load on the cavity, an all in one machined copper antenna including N connector inner contact, a movable copper outer line sliding inside the external body, a Vespel® ring to ensure concentricity between the antenna and the outer line, a ceramic ring with an EB weld between outer line and outer N connector, sliding RF contacts, and a displacement system and guidance rails made of stainless steel and brass to ensure positioning of the antenna in the cryogenic environment.

Validation tests of the prototype cavity tuning system are currently under way, while the first series coupler systems have been procured:

- 6 Cu plates available, 5 sputtered
- Actuating system fully redesigned to reduce torques and preserve alignment
- Hertzian contacts, no friction
- Two pre series systems are ready for cold test

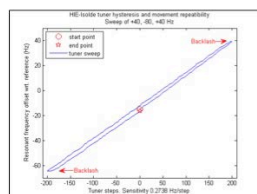
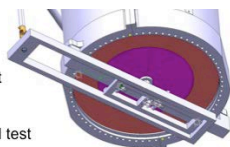


**Fig.10: Tuning System.**

- Couplers:
  - 2 pre series available (tested)
  - 5 series assembled and cleaned, last weld pending in AP
- Transmission system
  - Prototype tested in SM18
  - Design change done to allow easy replacement in the CM



**Fig.11: Coupler System.**

### Cryomodule Design:

The cavities will be grouped in common cryomodules with six cavities and two focussing solenoids for the low-beta cryomodules, and five cavities and one focussing solenoid for the high-beta cryomodules. Figure 12 shows a 3D model of the high-beta cryomodule. In order to minimise the drift length between cavities and the overall length of the machine a common vacuum was chosen for the beam and cryogenic insulation. The solenoids need to be aligned with stringent precision ( $\pm 0.15$  mm,  $\pm 1\sigma$  tolerance) and a system of independent adjustment under vacuum for the cavity and solenoid assembly is foreseen. A position monitoring system based on CCD cameras has been developed and validated. The active components will be cooled to 4.5 K in two stages using gaseous and liquid He. Insulation will be guaranteed by a heat screen at 75K. A vacuum of  $10^{-8}$  mbar after cryopumping is necessary for optimal operation. A detailed description of the high-beta cryomodule design can be found in [8].

### CM Design:

– Some items of the CM are still under design but are minor and should not interfere with the planned start of assembly.

#### Procurement of CM components:

- The fabrication of all long lead items (except Cavity/Solenoid Frame) is progressing well, but with little contingency for a start of assembly mid July. This is being vigorously followed-up.
- The contract of the Cavity/Solenoid Frame is being placed, however it is needed much later during the assembly process.
- Many smaller components are under fabrication or to be fabricated (i.e. heavy workload for CERN workshops and sub-contracting).

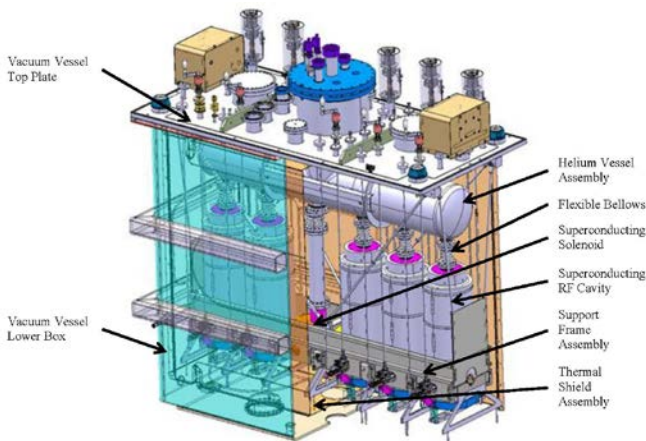


Fig. 12: General assembly view of the complete high-beta cryomodule.

training of assembly teams is to start mid June.

- Status:
  - Solenoid 1: weld of He vessel under way
  - Solenoid 2: coil wound and impregnated
  - Expected delivery dates: 30 April, 30 May

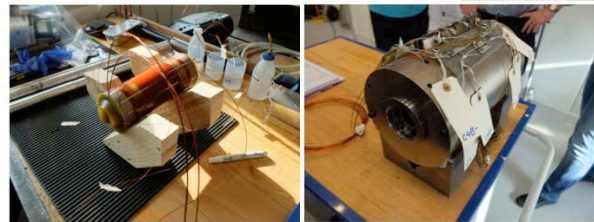


Fig. 14: Superconducting Solenoids.



- Contract tight but on schedule (a few NC, Change Requests from CERN → prompt reaction)
- Welding/welders qualifications done, assembly welding starting
- Delivery of 2 vacuum vessels planned by end of June (CM1 need mid July)

Fig. 13: Main Assembly Tooling.

Design/procurement of CM assembly tooling:

- Cavity/solenoid trolley drawings are being drafted. This item may become critical (needed mid-October), if the procurement is not started very soon.
- Other tools are still under design or to be fabricated.

The Assembly of CM1 (& CM2) is planned to start mid July and should last for 27 weeks (until first week of February 2015). This is rather challenging (no contingency) but credible in the case of no major problems. CM2 will largely profit from the experience of CM1.

The assembly process is mature, and procedures are under preparation. The

Main assembly tooling (manufacture through EN-MME)

- Railing system: installed
- Assembly Frame: structure fabricated, assembly/commissioning to start
- Multi-purpose trolley (with adaptation jigs): designed, fabrication to start
- Cavity/solenoid trolley: designed, drawing file in preparation

Fig. 15: Main Assembly Tooling.

**Planning and Operation:**

If the very tight and carefully planned schedule is respected, the various experiments currently receiving beams from ISOLDE will not suffer from the upgrade works. Installation of the remaining services such as power, ventilation and cooling, cabling will take place while the ISOLDE facility is running for the experiments. Installation works inside the experimental hall, such as the construction of the new tunnel, as well as the move of the existing Miniball experiment to its new position will also be carried out during this period of shutdown.

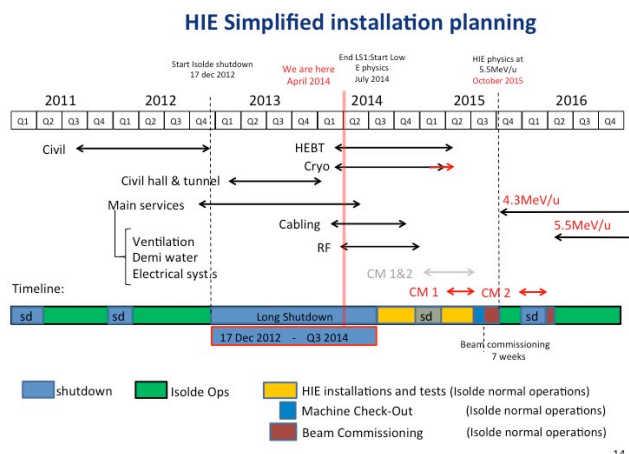


**Fig.16:** A simplified presentation of the HIE-ISOLDE planning

Start-up of the low energy (60keV/u) part of the ISOLDE facility excluding the REX post-accelerator is foreseen for July 2014. However at that moment the HIE-ISOLDE Linac and high-energy beam transfer line will still be under construction with the installation of the first beam transfer line elements starting during autumn of 2014. Installation of the first High-Beta Cryomodule is expected to take place during the second quarter of 2015. Beam commissioning is planned during summer 2015 and the start of the physics program at 4.3MeV/u (with only one CM) is expected in October 2015.

The second high-beta cryomodule will be installed during the ISOLDE shutdown in 2015-2016, increasing the beam energy to 5.5 MeV per nucleon.

The remaining two high-beta cryomodules will be installed in Phase 2, increasing the beam energy to 10MeV per nucleon, together with an additional bend to the high energy beam transfer line providing the users with a third experimental station (and possible connection of a storage ring at the back of the hall). A chopper line and the two low-beta cryo-modules completing the HIE-ISOLDE linac are foreseen for a later stage after 2018.

## Outlook:

The main technological options of the linac are now fixed and most components are under procurement. The high-energy beam transfer lines designs have been finalised and the components are being fabricated.

## Acknowledgements:

This brief report summarizes the work of several teams: The ISOLDE Collaboration, the HIE-ISOLDE Project team, and numerous groups at CERN within the accelerator and technology sector.

We acknowledge funding from the Swedish Knut and Alice Wallenberg Foundation (KAW 2005-0121) and from the Belgian Big Science program of the FWO (Research Foundation Flanders) and the Research Council K.U. Leuven.

We would like to acknowledge as well the receipt of fellowships from the CATHI Marie Curie Initial Training Network: EU-FP7-PEOPLE-2010-ITN Project number 264330.

[1] M. Lindroos, P.A. Butler, M. Huyse and K. Riisager. "HIE-ISOLDE" Nuclear Instruments and Methods in Physics Research B 266 (2008) 4687–4691.

[2] M.A. Fraser, R. M. Jones, and M. Pasini. "Beam Dynamics Design Studies of a Superconducting Radioactive Ion Beam Postaccelerator." Physical Review Special Topics - Accelerators and Beams 14, no. 2 (February 17, 2011): 020102.

[3] K. Riisager, P. Butler, M. Huyse, and R. Krücken. "HIE-ISOLDE: The scientific opportunities." CERN Report, CERN-2007-008 (November 22, 2007).

[4] D. Voulot, E. Bravin, M.A. Fraser, B. Goddard, Y. Kadi, D. Lanaia, A. Parfenova, M. Pasini, A. Sosa, F. Zocca, "HIE-ISOLDE SC linac: operational aspects and commissioning preparation", IPAC12.

A. Parfenova et al., "Design and Performance of the beam transfer lines for the HIE-ISOLDE Project", IPAC13.

- [5] E.D. Cantero et al., "Performance tests of a short Faraday Cup designed for HIE-ISOLDE", IPAC13.
- [6] K. Blaum, R. Raabe, "Storage ring facility at HIE-ISOLDE : Technical Design Report", CERN-INTC-2012-027 ; INTC-O-014
- [7] W. Venturini Delsolaro et al., "Nb Sputtered Quarter Wave Resonators For Hie Isolde", Proceedings of SRF2013.
- P. Zhang et al., "The tuning system for HIE-ISOLDE high- $\beta$  quarter-wave resonators", SRF2013
- A. Sublet et al., "Thin Film Coating Optimization for HIE-ISOLDE SRF Cavities: Coating Parameters Study and Film Characterization", SRF2013
- N. Jecklin et al., "Niobium Coatings for the HIE-ISOLDE QWR Superconducting Accelerating Cavities", SRF2013
- [8] N. Delruelle et al., "The high beta cryo-modules and the associated cryogenic system for the HIE-ISOLDE upgrade at CERN", Proceedings of CEC-ICMC conference, Anchorage, 17-21 June 2013.

*Yacine Kadi*

## [The HIE-ISOLDE Design Study: a roadmap for future upgrades.](#)

Initially instigated in the 2006 "HIE-ISOLDE: the technical options" CERN yellow report [1], it wasn't until 2011 that the Design Study team was set up and work really started. 2014 will see the publication of the Design Study Report, which addresses a four-fold increase in proton-beam power and proposals for improvements to the beam quality. The report will be divided into 4 sections: infrastructure, beam quality, targets and safety.

Although the infrastructure section is split up into various chapters, a holistic approach has to be taken when addressing infrastructure issues. A typical example is the issue of activated air. The radio-activation of air increases by a factor of approximately 1.5 when the proton-beam energy is increased from 1.4 GeV to 2 GeV. However, there is also a linear increase of air activation as a function of proton-beam intensity hence, with an increase from 2 $\mu$ A to 6.7 $\mu$ A, up to a five-fold total increase in air activation can be expected. One approach to reduce this factor is to regulate the flow of air throughout the target area during operation. By rendering the target area confinement air-tight, introducing air-locks and reducing the pulsed air flow, the extraction rate can be reduced from the current 2800m<sup>3</sup>h<sup>-1</sup> to as little as 900m<sup>3</sup>h<sup>-1</sup>. In parallel, Fluka simulations are being used to design improved shielding around the target and beam dump areas.

Both targets and frontends are covered in the target section simply because the modification of one has inherent consequences on the other. This is mirrored by the proposed modification of the beam-extraction system. The frontends have been subject to HT breakdowns owing to the incidental pollution of the extraction electrodes during operation, and the only

option has been to change the highly contaminated extraction electrode tip. The proposal implies mounting the extraction electrode tip inside the target unit. Acceleration would then be provided by a two-stage extraction process with one potential on the tip and a second on the fixed extraction electrode inside the frontend. Besides having the advantage of renewing the extraction electrode tip after each target change, this approach will also eliminate the existing mechanics of the electrode movement; a potential source of failure.

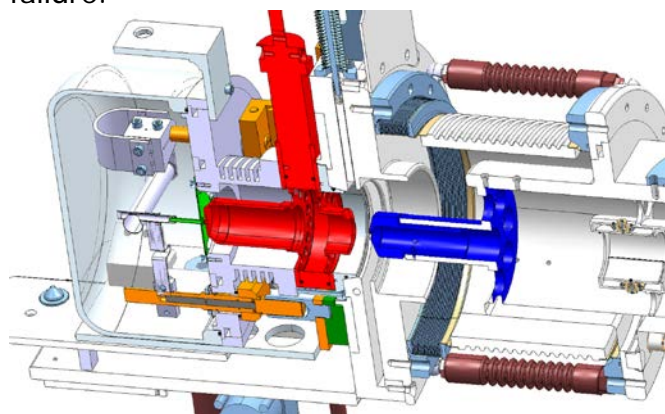


*Fig.1: A proposed pre-extraction prototype with the ion source (green) at 60kV, the intermediate electrode (red) at 57kV and the fixed frontend electrode (blue) at earth potential. Courtesy of J. Montano*

With an increase in proton-beam intensity, the load on the HT modulator will exceed the 5mA limit of the present design. Different types of high-voltage switches have been tested and preference has been given to commercial semiconductor switches. A test bench simulating a dynamic electrical load similar to the conditions generated by a p-beam impinging on a high-Z target has been built and tests continue.

The target team is also working on the thermodynamics of the target heating process. The goal is to reduce the required power for target heating and to produce a uniform heat distribution across the target

system to minimise radio-isotope production losses through temperature variations. Materials are also being addressed. Potential future target material samples of SiC and  $Al_2O_3$ , with a tailor-made microstructure using the ice-templating technique, have already been subjected to proton-beam bombardment at ISOLDE and CERN's HiRadMat facility [2]. These samples will undergo tests this year to characterize and evaluate their structure after irradiation. The beam quality section looks at the required upgrades and techniques for improving beam purity. This is addressed partly by improving the neutron converter design to further increase the ratio of specific neutron-rich fission isotopes to neighbouring isobars. Also being studied is the combination of an improved Radio Frequency Quadrupole Cooler and Buncher (RFQCB) placed before a High Resolution Mass separator magnet (HRMS) [3]. Mechanical modifications of the RFQCB are being simulated to optimize critical parameters relevant to beam transmission and emittance, such as internal helium gas pressures, and a new layout of the HRMS separator is proposed.

The beam quality section also includes the development of a High Energy Current and Compression (HEC<sup>2</sup>) EBIS charge breeder [4]. To exploit the full physics program at ISOLDE and match the demanding injection requirement of a possible future TSR@ISOLDE [5], the new EBIS design should provide an electron energy of up to 150KeV and an electron-beam density of  $10^4 \text{Acm}^{-2}$  in order to produce sufficiently highly charged ions within a given repetition rate. In collaboration with Brookhaven National Laboratory, preliminary tests of a new design are on-going and are producing promising results. A more detailed report on this development is presented in this Newsletter by A. Shornikov.

A Design Study Report would not be complete without a section on safety and although safety drives the issues already being addressed, this section will summarize and elaborate on safety aspects and outline any shortcomings. One example is the radiation levels recorded above the ISOLDE target area during operation. While safety is assured by fencing off the area, further investigations into the improvement of shielding will no doubt be required.

Finally, to complete the report, the boundary conditions in terms of infrastructure and operations will be balanced against both cost and safety. A summary of each section including projected budgets and schedules will be presented.

[1] M. Lindroos, T. Nilsson, CERN Yellow Report, CERN-2006-013.

[2] Czapski M. et al. NIM B 317 (2013) 385-388

[3] Shornikov A. et al. NIM B 317 (2013) 395-398

[4] Babcock C. et al. NIM B 317 (2013) 484-487

[5] M. Grieser. et al. Eur. Phys. J. Special Topics 207, 1-117 (2012)

*Richard Catherall, ISOLDE Technical Coordinator*

### [First experiments with electron beams for a future HIE-ISOLDE charge breeder](#)

The HIE-ISOLDE upgrade gives the user community ample opportunities for new experiments. To fully take advantage of the intensive and high energy beams from the superconducting linac a matching injection system for highly charged ions (HCI) is needed. The charge breeding system should enable pulse repetition rates up to 100 Hz, while maintaining transmission efficiency and beam quality.

The only type of charge breeder capable of delivering such beams is based on the Electron Beam Ion Source (EBIS) technology, similar to REXEBIS currently in service at ISOLDE. However, the design parameters required to meet the user expectations imply a major upgrade of the breeder. In fact, the breeder should be completely replaced with a new one featuring higher electron-beam energy, electron current, current density and confining magnetic field. The specified design parameters for HIE-ISOLDE exceed by far operational parameters of any existing EBIS-like device. Therefore, a comprehensive design and feasibility study with emphasis on experimental realization is required. This work has been started within the framework of the HIE-ISOLDE design study.

The key component of the new breeder is a High Energy, Current and Compression (HEC<sup>2</sup>) electron beam. The beam provides both the ion confinement and ionization. The high compression beam needs to be produced by a gun, which is different from the immersed flow gun such as used at REXEBIS. The fundamental difference is the electron beam launching. In immersed flow guns the electron beam is produced in a relatively strong magnetic field and later compressed by increased magnetic field in the trapping volume. This is a stable and reliable technique, however, it is limited by the emission current density at the cathode. Realistically it does not allow current densities above 700 A/cm<sup>2</sup> for any available combination of cathode material and superconducting magnet.

In high compression guns, as used in HEC<sup>2</sup>, the electron beam is generated in a region shielded from the magnetic field. The beam is then electrostatically compressed to its minimum size and at this point injected in a rapidly increasing magnetic field (see Fig.1). In this way electrostatic and magnetic

compression factors will be multiplied yielding much higher current densities in the order of thousands and theoretically tens of thousands of  $A/cm^2$ .

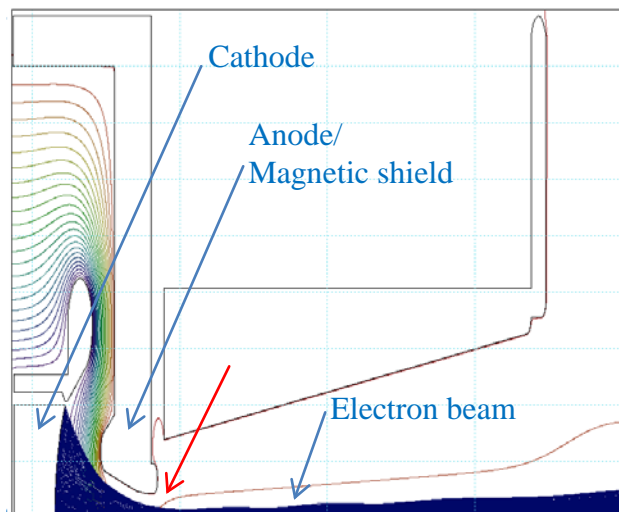


**Fig.1:** Generation of high compression electron beam in HEC<sup>2</sup> electron gun. The red arrow indicates the injection into a 0.2 T magnetic field which will be gradually increased to 5 T after a short drift region with lower field.

To succeed, it requires precise matching of electric and magnetic focusing systems and very careful shielding of the magnetic field lowering it from 5 T in the trapping region to a few  $10^{-4}$  T at the cathode surface.

During 2013 the CERN team in cooperation with Brookhaven National Lab Advanced Ion Source group carried out the construction, installation and early commissioning of a prototype electron gun for HEC<sup>2</sup>. The gun is designed by BNL [1], built at CERN and commissioned by the joint team on the BNL test stand TEBIS (Fig. 2). On the occasion of the first commissioning run in Nov 2013 the gun demonstrated promising results of 1.5 A of extracted current at 30 keV electron energy (Fig. 3), to be compared with normal operation of 0.2 A and 5 keV at REXEBIS. The achieved current was limited by a load current on the biasing power supplies originating either from returned

electron flux or a glowing discharge. Both will be addressed in the next runs.



**Fig.2:** BNL TEBIS with installed HEC<sup>2</sup> electron gun being prepared for the operation.

The experiments will be continued in 2014 to define the efficiency of the electron beam compression scheme and advance towards the target values for both parties (CERN 5A, 40 keV, 10  $kA/cm^2$  and BNL 10A, 20 keV, 5  $kA/cm^2$ ). A set of beam diagnostic tools is currently being built at CERN to enhance the beam control and manipulation. The implementation of the beam diagnostics will let us move from solely operating the electron beam, to studies of the actual charge breeding of intensive beams.

This development is also a first step towards an even more futuristic HEC<sup>2</sup> II breeder needed to provide optimal injection into a heavy ion storage ring, TSR@ISOLDE, should it be installed behind the HIE-ISOLDE linac [2]. Some of the planned experiments rely on a possibility to inject bare and few-electron configurations of medium-Z and heavy ions into the ring. Unlike at FSR at GSI the energy of HIE-ISOLDE linac is far below the energy which allows production of such ions by foil strippers. The only practical solution would be to have an EBIS even more powerful than HEC<sup>2</sup>.



**Fig.3:** A 7 ms current pulse of at maximum 1.5 A (pink) extracted from the HEC<sup>2</sup> gun.

By sheer coincidence the electron current density required for a 100 Hz injection rate into the HIE-ISOLDE linac for  $A/q = 4.5$  ions is very close to the one needed for production of few electron configurations of heavy ions at a 0.5-1 Hz rate [3]. This makes the HEC<sup>2</sup> gun an ideal benchmark for HEC<sup>2</sup> II. Nevertheless, an electron current density in excess of 10 kA/cm<sup>2</sup> would benefit HEC<sup>2</sup> II as it not only allows matching the injection pace of the storage ring, but is also crucial to counteract charge-exchange recombination with neutral atoms inside the charge breeder. Even at best practically achievable vacuum, only a highly compressed electron beam allows reaching highest ionization states. From the lowest to the highest charge states the electron-impact ionization cross-section decreases 7 orders of magnitude, while the charge exchange cross-section with neutrals gains 5 orders. Eventually, even in 10<sup>-10</sup> mbar vacuum the probability of ionization is equal to recombination for 10 kA/cm<sup>2</sup> electron beams. The second fundamental requirement for the highest charge states is the electron beam energy. The HEC<sup>2</sup> II breeder should have an electron-beam energy up to 150 keV, enough to ionize lowest shells of heavy

elements and counteract the competing radiative recombination process [3]. HEC<sup>2</sup> II also puts special emphasis on vacuum requirements and means of emittance growth control, because it must store the ions for as long as a few seconds [3].

As a potentially important component of a future EURISOL facility a continuation of the HEC<sup>2</sup> investigation was favoured by the EURISOL JRA within ENSAR2 framework.

[1] Pikin et al, Rev Sci Instrum. 2013 84(3):033303. doi: 10.1063/1.4793773.

[2] Grieser et al, The European Physical Journal Special Topics, 2012, 207, 1, pp 1-117, doi: 10.1140/epjst/e2012-01599-9

[3] Shornikov et al, I NIM B, 2013, 317, B, pp395-398, doi 10.1016/j.nimb.2013.06.030

*Andrey Shornikov for the EBIS team*

## (CERN-)MEDICIS

If you ask someone on the street "Do you know anything about *MEDICIS*?" they would probably think you were referring to the Italian *famille de MEDICIS* which became famous during the Renaissance. However, native English speakers would simply refer to the family *MEDICI*, and not make any connection with *CERN-MEDICIS*. A first step towards putting us back on the right track comes from an investigation with a popular web-search engine, looking for example for images related to *CERN-MEDICIS*, Fig.1. With careful examination of this photograph, one may find one or two familiar faces, and reference to some ground-breaking activities. This looks, however, to be far from MR-TOF-assisted <sup>54</sup>Ca mass measurement, Coulex of <sup>224</sup>Ra at REX-ISOLDE and Rydberg series

determination on  $^{205}\text{At}$  radioactive ion beams. Investigating further, it seems that a world-renown oncologist, a medical radiologist from Lausanne hospital and a directorate member from Geneva hospital had joined efforts with the CERN DG. As such, this could already have been seen as "ground-breaking". But more activity related to *MEDICIS* was to follow:



**Fig. 1:** Ground-breaking ceremony for CERN-MEDICIS on September 4<sup>th</sup>, 2013 (reprinted from Ref. 1).

If you happen to pass by ISOLDE on route Goddard, a new building has seen the light of day extending the present class A target building, Fig. 2. No windows towards the outside are to be seen, complying with the present regulations for buildings with regards to radiological protection matters. A temporary access will be available to set-up additional equipment this year, like the ventilation services or target storage, while ISOLDE resumes its operation this summer. The building, and its ventilation system, will be connected to the existing building 179 during the next winter shutdown, keeping common access doors. While most of the external walls are made of classical concrete, parts of the structures inside must efficiently protect against the neutron and gamma stray radiation fields originating from the targets under or after exposition to the proton beam irradiation. Here, we use a very particular type of heavy concrete, dark grey or black that is made of magnetite stones instead of the traditional silicates, as

seen on the Figure 2 insert. The concrete used for the walls, at a weight of 4 tons/m<sup>3</sup>, gives a total of nearly 500 tons together with the heavy lead shielding of the hot-cells, which would truly be breaking the ground, if not carefully addressed.



**Fig. 2:** Building as seen on the CERN-MEDICIS construction site, taken on February 4<sup>th</sup>, 2014. Insert: magnetite stone and loaded cement used to make heavy concrete shielding walls (not yet to be seen on the picture).

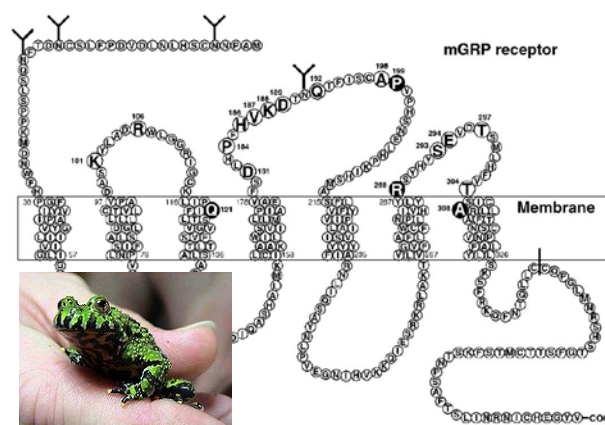


**Fig. 3:** Schematic secondary structure of the mammalian gastrin releasing peptide receptor, a G-protein coupled receptor naturally present in the digestive system and overexpressed in specific cancer tissues such as in prostate cancers. A radio-peptide, analog of the bombesin, a protein found in the *bombina-bombina* frog skin (seen in the insert), is shown to specifically bind to the mGRP with high specificity.

Logically the next question coming to mind would be: what is this new building useful for?

ISOLDE has pioneered and provided multi-user capabilities, such as the parallel collections at GLM and GHM experimental beam lines while beams are delivered at GPS. In a sense, *CERN-MEDICIS* will enlarge this capability, because it will recycle the proton beam that would otherwise become lost in the beam dump. It will operate an independent irradiation target station, related to the units we operate for Isolde, but modified for the purpose of producing high quantities of long-lived isotopes for medical applications. Indeed, the mass-separation step will only occur when the target unit is recuperated from the irradiation point using a rail conveyor system and a robot, and is set onto a dedicated offline isotope mass separator in the building extension. The mass separator will be recuperated from LISOL and refurbished. The collected isotopes are subsequently shipped to medical research laboratories where the synthesis of the radiological biomolecules is carried out, prior to testing in biological models. As a proof of feasibility, a test collection of  $^{152}\text{Tb}$  took place at ISOLDE in 2012 and shipped to Prof F. Buchegger and J. Prior at CHUV in Lausanne, active members of the *CERN-MEDICIS* medical collaboration (HUG, ISREC-EPFL, CHUV). Tests were carried out on nude mice grafted with PC3 prostate cancer tumours which lead to important new results [2]. Treatments trials with therapeutic isotopes will follow as soon as possible. The commissioning of the facility should start in a year, and test collections at the end of 2015 or beginning of 2016.

To summarise, *CERN-MEDICIS – Medical Isotopes collected from Isolde* – is an upcoming new facility and already an enlarging collaboration [3].

- [1] CERN-Courier, 53 (9), p. 37.  
<http://cerncourier.com/cws/article/cern/55005>.
- [2] F. Bucchegger et al., submitted to the Swiss Nuclear Medicine society meeting (2014).
- [3] R. Augusto et al., CERN Acc Report, in the press.

*T. Stora for the CERN-MEDICIS collaboration*

## Experiment reports:

### IS453: Emission Channeling with Short-Lived Isotopes (EC-SLI)

June/July 2013 carried a lucky spell for the EC-SLI collaboration, with three of our young researchers winning awards at major conferences in Materials Science.

First, Lino Pereira, at that time post-doc at IKS/KULeuven in Belgium, where he was recently appointed as Assistant Professor, was runner up in the "Young Researcher for Best Manuscript Competition" (sponsored by Elsevier BV) at the 21<sup>st</sup> International Conference on Ion Beam Analysis in Seattle, for his contribution on "Emission channeling studies on a challenging case of impurity lattice location: cation versus anion substitution in transition-metal doped GaN and ZnO", cf. ISOLDE Newsletter 2012.

Then, Ligia Amorim, PhD student also at IKS, won the "Award for Best Student Oral Presentation" at the 17<sup>th</sup> International Conference on Radiation Effects in Insulators in Helsinki, for her talk on "Lattice sites of implanted Mg in the group-III nitrides", cf. ISOLDE Newsletter 2013.

Last but not least, Daniel Silva, PhD student from Porto University, won the prestigious J.W. Corbett prize at the 27<sup>th</sup> International Conference on Defects in Semiconductors in Bologna. The topic of his contribution was "Influence of the doping on the lattice sites of Fe in Si", and presented clear evidence that the preferred lattice location of Fe changes with the doping of the material (Fig. 1, [1]). While in  $n^+$ -type Si Fe prefers displaced bond-centered (BC) sites for annealing temperatures up to 600°C, changing to ideal substitutional sites above 700°C, in  $p^+$ -type Si, Fe prefers to be in displaced tetrahedral interstitial positions after all annealing steps. The dominant lattice sites of Fe in  $n^+$ -type Si therefore seem to be well characterized for all

annealing temperatures by the incorporation of Fe into vacancy-related complexes, either into single vacancies which leads to Fe on ideal substitutional sites, or multiple vacancies, which leads to its incorporation near BC sites. In contrast, in  $p^+$ -type Si, the major fraction of Fe is clearly interstitial (near-T or ideal T) for all annealing temperatures. The preference of Fe for interstitial sites in  $p^+$ -Si results from its 1+ charge state in that material, which also favours the formation of  $Fe^+B^-$  pairs. In intrinsic and  $n^+$ -Si, on the other hand, Fe, as positive  $Fe^+$  or neutral  $Fe^0$ , seems to combine preferentially with Si (multiple) vacancies that tend to be negatively charged for that doping type.

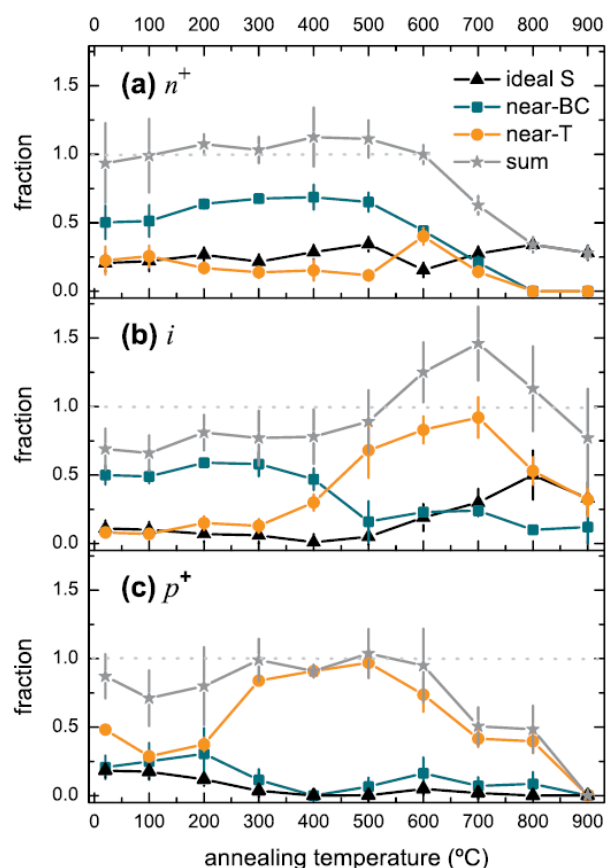


**Fig.1:** Annealing temperature dependence of the lattice site fractions of  $^{59}\text{Fe}$  in different doping types of Si, from [1].

[1] D.J. Silva, U. Wahl, J.G. Correia, and J.P. Araújo, J. Appl. Phys. 114 (2013) 103503.

*Ulrich Wahl (for the EC-SLI Collaboration)*

## IS471: CRIS makes it to PRX

The CRIS experiment at ISOLDE was very successful at the end of the last running campaign. The data collected on the neutron-deficient francium isotopes pushed the limit of knowledge to  $^{202}\text{Fr}$  [1], two isotopes further than the state-of-the-art collinear laser fluorescence spectroscopy [2], with a beam intensity as low as 100 ions per second.

Beyond the high sensitivity of the resonance ionization technique, one of the strengths of CRIS lies in ion identification. In the same vein as the combination of the RILIS with the Windmill for the in-source laser spectroscopy programme [3], the CRIS experimental setup includes a decay spectroscopy station (DSS), compatible with the UHV requirements of the CRIS beam line [4]. It proved essential for the understanding of the case of  $^{202,204}\text{Fr}$  where isomers are found and hyperfine structures overlap, even if probed with the highest resolution.

As a follow up to the original Letter [1], we proposed an extended article describing this novel approach, combining the high sensitivity of resonance ionization, the Doppler-free resolution of the collinear geometry, and the identification power of the DSS. It also reports on the magnetic dipole moments of the neutron-deficient francium isotopes, completes the systematics of the charge radii, as well as presents the first measurement of the branching ratios in the decay of the  $(10^-)$  isomer in  $^{204}\text{Fr}$ . It was recently accepted as the first nuclear physics contribution to the new APS journal Physical Review X [5].

This young, high-impact, fully open-access, and broad-scope journal aims at publishing and broadly disseminating cutting-edge experimental and theoretical work that opens new prospects and research avenues. As ISOLDE has a long tradition in this line of research, I invite you all to keep a close eye on PRX in the times to come! <http://journals.aps.org/prx>

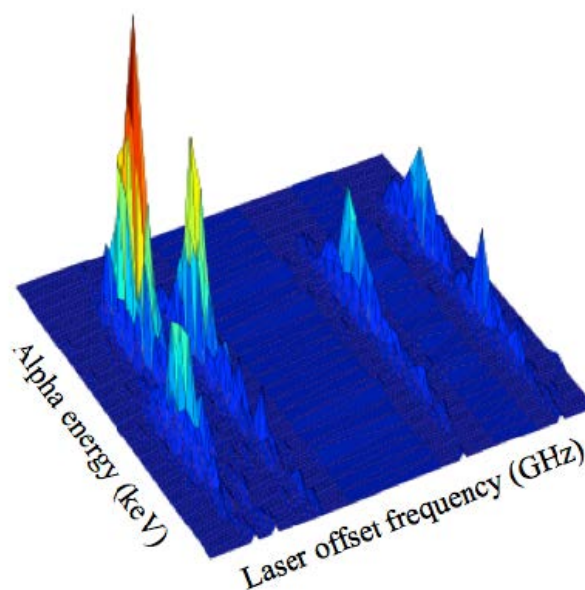


**Fig.1:** 3D representation of the  $^{204}\text{Fr}$  data from October 2012. Alpha-decay spectra were acquired at each laser frequency, hereby revealing the different decay patterns and the hyperfine structure simultaneously.

The data analysis of the neutron-rich francium isotopes at the border of the region of shape reflexion asymmetry is completed and a dedicated publication is in preparation [6]. The magnetic dipole moments are the key to understanding the influence of the intruder  $\pi s_{1/2}$  orbital, also of interest for the neutron-deficient isotopes.

- [1] K.T. Flanagan et al., PRL 111 (2013) 212501
- [2] A. Voss et al., PRL 111 (2013) 122501
- [3] A.N. Andreyev & T.E. Cocolios, INTC-SR-029
- [4] M.M. Rajabali et al., NIMA 707 (2013) 35-39
- [5] K.M. Lynch et al., PRX in print  
<http://arxiv.org/abs/1402.4266>

[6] I. Bundošević et al., Letter in preparation

*T.E. Cocolios for the CRIS Collaboration*

## IS474: Fast-timing study of neutron-rich Fe isotopes

The region below  $^{68}\text{Ni}$  has drawn considerable attention recently, both from an experimental and theoretical point of view.  $^{68}\text{Ni}$  exhibits some of the properties of a double magic nucleus, such as a high  $2_1^+$  energy and low  $B(E2)$  value. However  $^{66}\text{Fe}$  (two protons below  $^{68}\text{Ni}$ ) and  $^{64}\text{Cr}$  (four protons below) do not show such behaviour, having instead low-lying  $2_1^+$  states and high  $B(E2)$  values (see Fig.1), which can be interpreted as an enhanced quadrupole collectivity. Shell model calculations have shown that this effect can only be reproduced by including the deformed intruder neutron orbitals  $\nu g_{9/2}$  and  $\nu d_{5/2}$  [1].

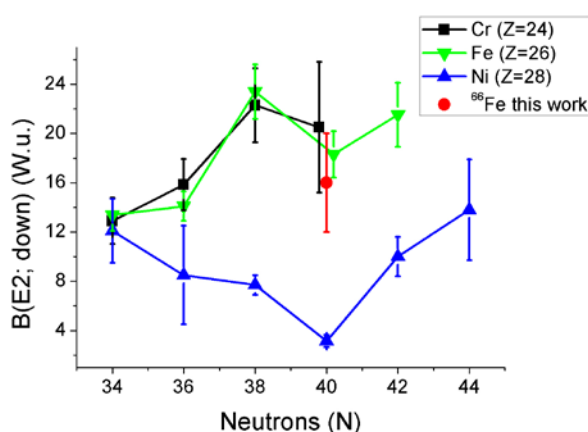


**Fig.1:**  $B(E2)$  systematics of the  $2_1^+ \rightarrow 0_1^+$  transitions in the region below  $^{68}\text{Ni}$ . In red the value for  $^{66}\text{Fe}$  from the lifetime measurement in this work.

In order to characterize the systematics of this region, a very successful Advanced Time Delayed (ATD)  $\beta\gamma\gamma(t)$  [2] experiment was performed during August 2010 at

ISOLDE (IS474) on  $^{59-66}\text{Mn}$  isotopes. Protons at 1.4 GeV from the PS Booster impacted in a  $98.4 \text{ g/cm}^2 \text{ UC}_x$  target. Mn isotopes were ionized using the resonance ionization laser ion source (RILIS). The isotopes were mass separated by the GPS and implanted in an aluminium foil at the experimental area. The experiment setup consisted of five detectors: a thin NE111A plastic for  $\beta$  particles, two very fast truncated-cone shaped  $\text{LaBr}_3(\text{Ce})$  and two HPGe with 60% relative efficiency. The analysis of the data has yielded valuable results so far on  $^{63,65,66}\text{Fe}$ . The lifetime of the  $2_1^+$  state in  $^{66}\text{Fe}$  has been re-measured, yielding a transition rate in very good agreement with recent values (see Fig.1). The level schemes of  $^{63,65}\text{Fe}$  nuclei have been greatly expanded and the energy of the  $9/2^+$  isomers in these nuclei have been measured for the first time (see Fig.2). The lifetimes or upper limits of several low-lying states have been

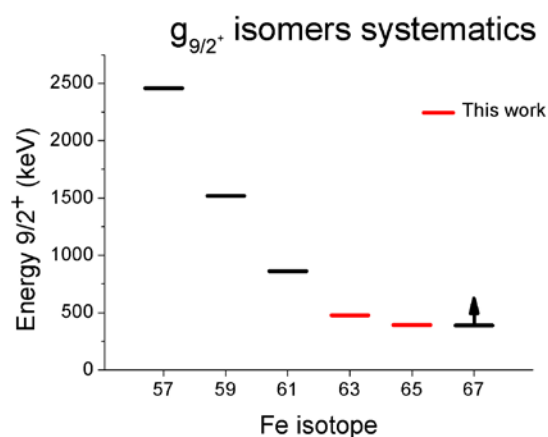


**Fig.2:** Energy of the  $g_{9/2}^+$  isomers of the odd Fe nuclei. In red the two new energy values from this work.

measured as well. For the first time the population of excited levels following the  $\beta$ -n decay of these nuclei has been observed and their  $P_n$  re-measured with increased precision.

These and other results have been included in the PhD Thesis work by the author, which was successfully defended in September 2013 [3].

[1] S.M. Lenzi et al. Phys. Rev. C, 82:054301, 2010.

[2] H. Mach, NIM A 280, 49 (1989).

[3] <https://cds.cern.ch/record/1645676>

*Bruno Olaizola for the IS474 Collaboration*

## IS475: Pear-shaped nuclei studied at ISOLDE

Coulomb excitation is an important tool for exploring the collective behaviour of deformed nuclei that gives rise to strong enhancement of the probability of transitions between states. Whereas E2, E1 and magnetic dipole (M1) transition probabilities dominate in the electromagnetic decay of nuclear states, and hence can be determined from measurements of the lifetimes of the states, E2 and E3 transition moments dominate the Coulomb excitation process allowing these moments to be determined from measurement of the cross-sections of the states, often inferred from the  $\gamma$ -rays that de-excite these levels. The E3 transition moment is collective in behaviour and is insensitive to single-particle effects, as it is generated by coherent contributions arising from the quadrupole-octupole shape such as illustrated in Figure 1 for  $^{224}\text{Ra}$ . The E3 moment is therefore an observable that should provide direct evidence for enhanced octupole correlations (pear-shapes) and, for deformed nuclei, can be related to the intrinsic octupole deformation parameters.

It is only comparatively recently that the technique has been extended to the use of accelerated beams of radioactive nuclei such as those from REX-ISOLDE. In order to

study octupole correlations in heavy nuclei,  $^{220}\text{Rn}$  and  $^{224}\text{Ra}$  ions were produced by spallation in a thick uranium carbide target bombarded by protons from the CERN PS Booster. The ions were post-accelerated in REX-ISOLDE to an energy of 2.8 MeV per nucleon and bombarded secondary targets

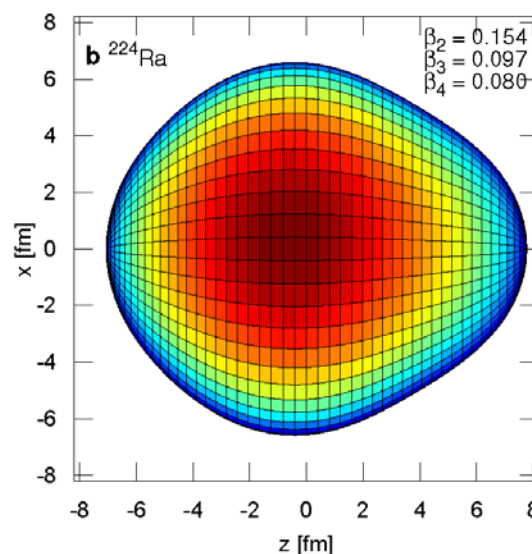


**Fig.1:** Representation of the shape of  $^{224}\text{Ra}$ ; see reference [1] for details.

of  $^{60}\text{Ni}$ ,  $^{112,114}\text{Cd}$ , and  $^{120}\text{Sn}$ . The  $\gamma$ -rays emitted following the excitation of the target and projectile nuclei were detected in MINIBALL. The results from these experiments were recently published in Nature [1], accompanied by a News & Views article [2] and the main cover image/story for the issue as well as the thesis of Liam Gaffney [3].

The measured values of the E2 and E3 matrix elements are all consistent with the geometric predictions expected from a rotating, deformed distribution of electric charge. Figure 2 compares the experimental values of  $Q_\lambda$  derived from the matrix elements connecting the lowest states for nuclei near  $Z = 88$  and  $N = 134$  measured by Coulomb excitation. It is striking that while the E2 moment increases by a factor of 6 between  $^{208}\text{Pb}$  and  $^{234}\text{U}$ , the E3 moment changes by only 50% in the entire

mass region. Nevertheless, the larger  $Q_3$  values for  $^{224}\text{Ra}$  and  $^{226}\text{Ra}$  indicate an enhancement in octupole collectivity that is consistent with an onset of octupole deformation in this mass region. On the other hand,  $^{220}\text{Rn}$  has similar octupole strength to  $^{208}\text{Pb}$ ,  $^{230,232}\text{Th}$  and  $^{234}\text{U}$ , consistent with it being an octupole vibrator.

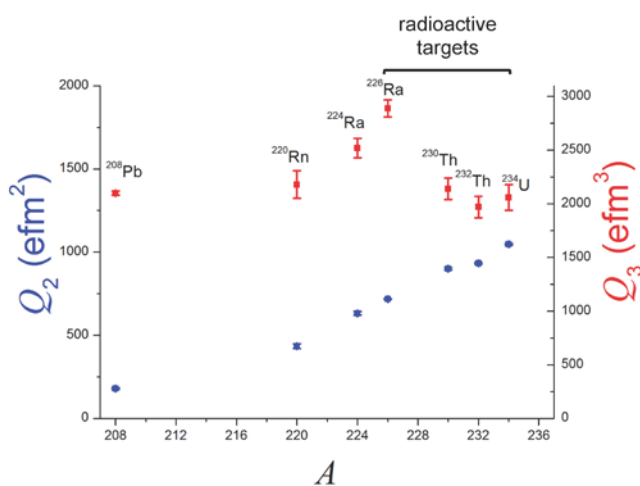


**Fig.2:** Measured electric-quadrupole and octupole moments for nuclei in the actinide region. The octupole moment remains almost constant over the mass range, with only  $^{224,226}\text{Ra}$  showing an enhancement.

The values of  $Q_{\lambda}$ , deduced from the measured transition matrix elements, are plotted in figure 3 as a function of  $N$ . The measured  $Q_2$  values are in good agreement with several theoretical calculations, especially for  $^{224}\text{Ra}$  and the heavier radium isotopes. The trend of the experimental data for  $Q_3$  is that the values decrease from a peak near  $^{226}\text{Ra}$  with decreasing  $N$  (or  $A$ ), which is in marked contrast to the predictions of the cluster model calculations [4]. It is also at variance with the Gogny HFB mean-field predictions of a maximum for  $^{224}\text{Ra}$  [5]. As can be seen, the relativistic mean field calculations [6] predict that the maximum value of  $Q_3$  occurs for radium isotopes between  $A = 226$  and  $230$ , depending on the parameterization, and

Skyrme Hartree-Fock calculations [7] predict that  $^{226}\text{Ra}$  has the largest octupole deformation, consistent with the data.

Atoms with octupole-deformed nuclei are very important in the search for permanent atomic electric-dipole moments (EDMs). The

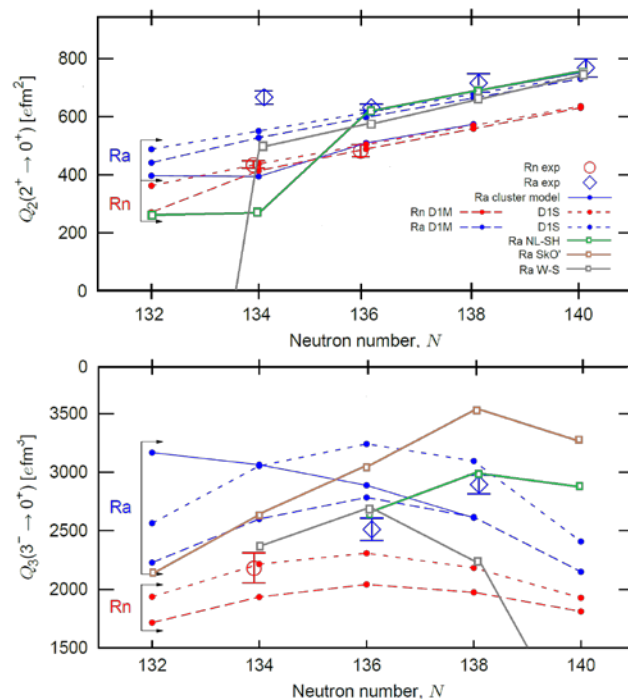


**Fig.3:** Values of  $Q_2$  and  $Q_3$  for low-lying transitions as a function of  $N$ . Measured [1] values are compared to various theoretical models: cluster model [4], Gogny HFB with D1S and D1M parameterizations [5], relativistic mean field ('NL-SH' [6], Skyrme HF ('SKO') [7] and shell-corrected liquid drop models ('W-S' [8]).

observation of a non-zero EDM at the level of contemporary experimental sensitivity would indicate time-reversal (T) or equivalently charge-parity (CP) violation due to physics beyond the standard model. In fact, experimental limits on EDMs provide important constraints on many proposed extensions to the standard model. For a neutral atom in its ground state, the Schiff moment (the electric-dipole distribution weighted by radius squared) will have enhanced values in odd- $A$  octupole-

deformed nuclei owing to the presence of the large octupole collectivity and the occurrence of nearly degenerate parity doublets that naturally arise if the deformation is static (see, e.g. [9]). Because a CP-violating Schiff moment induces a contribution to the atomic EDM, the sensitivity of the EDM measurement to CP violation over non-octupole-enhanced systems such as  $^{199}\text{Hg}$  [10], currently providing the most stringent limit for atoms, can be improved by a factor of 100-1000 [9]. Essential in the interpretation of such limits in terms of new physics is a detailed understanding of the structure of these nuclei. Experimental programmes are in place to measure EDMs in atoms of odd-A Rn and Ra isotopes in the octupole region but so far there is little direct information on octupole correlations in these nuclei. These measurements of  $Q_3$  values in  $^{220}\text{Rn}$  and  $^{224}\text{Ra}$  are consistent with suggestions from the systematic studies of energy levels [11] that the even-even isotopes  $^{218-222}\text{Rn}$  and  $^{220}\text{Ra}$  have vibrational behaviour while  $^{222-228}\text{Ra}$  have octupole-deformed character. It is concluded that the parity doubling condition that leads to enhancement of the Schiff moment is unlikely to be met in  $^{219,221}\text{Rn}$ . On the other hand  $^{223,225}\text{Ra}$ , having parity doublets separated by  $\sim 50$  keV will have large enhancement of their Schiff moments.

The publication in Nature generated considerable media attention. Some examples are given in:

<http://ns.ph.liv.ac.uk/pab/ExpProgWebPage/Pear-nuclei-press.htm>. CERN dedicated two Google Hangouts to this story as well as the astatine ionisation breakthrough, see:

<http://youtu.be/x8Jdu9O2RhU>, and

<http://youtu.be/eEUPvii2UcQ>.

Finally, the UK magazine Physics World selected the nuclear pear-shape measurements as one of the top 10 breakthroughs of 2013, see:

<http://iopublishing.org/newsDetails/top-10-physics-breakthroughs-for-2013-announced>

- [1] L. P. Gaffney et al., *Nature* 497, 199 (2013).
- [2] C. J. Lister and J. Butterworth, *Nature* 497, 190 (2013).
- [3] L. P. Gaffney, Octupole Collectivity in  $^{220}\text{Rn}$  and  $^{224}\text{Ra}$ , *University of Liverpool*, (2012).
- [4] T. M. Shneidman et al., *Phys. Rev. C* 67, 014313 (2003).
- [5] L.M. Robledo and G.F Bertsch, *Phys. Rev. C* 84, 054302 (2011).
- [6] K. Rutz et al., *Nucl. Phys. A* 590, 680 (1995).
- [7] J. Engel et al., *Phys. Rev. C* 68, 025501 (2003).
- [8] W. Nazarewicz et al., *Nucl. Phys. A* 429, 269 (1984).
- [9] J. Dobaczewski and J. Engel, *Phys. Rev. Lett.* 94, 232502 (2005).
- [10] W.C. Griffith et al., *Phys. Rev. Lett.* 102, 101601 (2009).
- [11] J.F.C. Cocks et al., *Nucl. Phys. A* 645, 61 (1999).

*Peter A. Butler and Liam P. Gaffney (for the IS475 Collaboration)*

## IS476: The $\beta$ -delayed three-proton decay of $^{31}\text{Ar}$

The IS476 experiment that took data in 2009 studied the  $\beta$ -delayed proton decays of  $^{31}\text{Ar}$  using six segmented Si-detectors in telescopes in cube formation for particle detection and two Miniball germanium detectors for detection of  $\gamma$ -rays. On average we had a yield of one  $^{31}\text{Ar}$  ion per second made from a CaO powder target with a VADIS ion-source. A complete description of the setup can be found in [1,2].

IS476 has resulted in two papers; one published [1] and one under review [2]. Ref. [1] focused on the levels of the  $\beta$ -

daughter  $^{30}\text{S}$  just above the proton threshold relevant for astrophysics. The main article [2] includes a new method for determination of the spin of low-lying levels in  $^{30}\text{S}$  using proton-proton angular correlations from the  $\beta 2p$ -decay of  $^{31}\text{Ar}$ . An improved determination of the half-life and the Fermi  $\beta$ -strength is given as well as a presentation of the strongest  $\gamma$ -transitions in the decay of  $^{33}\text{Ar}$  (used for calibration) including a decay of the IAS, which was not previously identified.

The analysis of IS476 revealed a new decay branch:  $\beta 3p$ -branch, which has only been seen in two other isotopes so far:  $^{45}\text{Fe}$  [3] and  $^{43}\text{Cr}$  [4,5]. It was only recently discovered in the decay of  $^{31}\text{Ar}$  [6]. IS476 provides, for the first time, a good energy and angular resolution, so that this decay mode can be studied in spectroscopic detail. Fig. 1 shows the  $Q_{3p}$ -value calculated for the multiplicity-three events. The dashed line is a simulation (downscaled) of the  $3p$ -decay of the isobar analogue state (IAS).

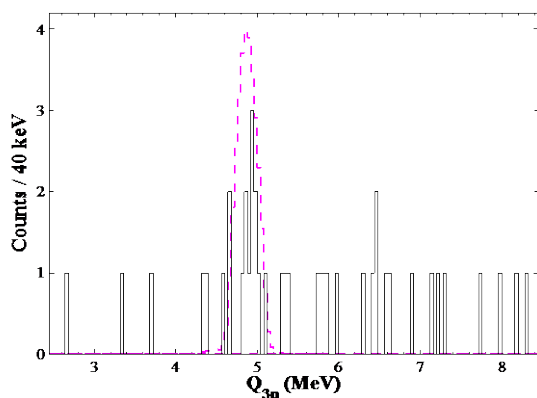


**Fig. 1:** The  $Q_{3p}$ -value calculated for multiplicity-three events. The dashed line shows a (downscaled) simulation of the  $3p$ -decay from the IAS.

This decay is clearly seen in the data and a total branching ratio of 0.039(19) % (not including the 11 % uncertainty from the normalisation) is deduced [2].

The good energy and angular resolution of the individual protons also makes it possible to study the decay mechanism of the  $3p$ -

decay [2]. We found that all the decays can be explained as sequential, but a simultaneous component cannot be excluded. Decays through a state in  $^{29}\text{P}$  at 3447.6(4) keV, just 699 keV above the proton threshold, are clearly identified for the IAS decays and strong indication of transitions through the next level at 4080.5(3) keV is also evident.

As can be seen in Fig. 1 only approximately half of the  $3p$ -events stem from the IAS, while the rest stem from levels in  $^{31}\text{Cl}$  above the IAS. From these events an improved determination of the Gamow-Teller  $\beta$ -strength is found [7]. A comparison with theoretical calculations shows that almost all the predicted strength can be identified in the  $1p$ -,  $2p$ - and  $3p$ -decay.

[1] G.T. Koldste *et al.*, Phys. Rev. C 87 (2013) 055808.

[2] G.T. Koldste *et al.*, arXiv:1402.4620 (2014), submitted to Phys. Rev. C.

[3] K. Miernik *et al.*, Phys. Rev. C 76 (2007) 041304.

[4] M. Pomorski *et al.*, Phys. Rev. C 83 (2011) 014306.

[5] L. Audirac *et al.*, Eur. Phys. J. A 48 (2013) 179.

[6] M. Pfützner *et al.*, GSI Scientific Report 147 (2013).

[7] G.T. Koldste *et al.*, *Precise measurement of the  $^{31}\text{Ar}$   $\beta$ -delayed three-proton decay* unpublished.

*G. T. Koldste (for the IS476 Collaboration)*

## IS495: Coulomb excitation of $^{140}\text{Sm}$

The aim of IS495 was to deduce B(E2) values and quadrupole moments of low lying states in neutron-deficient  $^{140}\text{Sm}$  using multi-step Coulomb excitation.

The particle-gamma coincidence experiment was performed in 2012 using the MINIBALL HPGe array coupled to an annular DSSD detector. The RILIS ionization method was used to produce a quasi-pure beam of radioactive  $^{140}\text{Sm}$ . The beam was accelerated to 2.85 A MeV and scattered on a 2 mg/cm<sup>2</sup> thick  $^{94}\text{Mo}$  target with an intensity of  $2 \cdot 10^5$  ions per second. Both projectiles and recoil particles were detected in the current experiment.

The figure shows the background-subtracted gamma ray spectrum Doppler corrected for the velocity of the  $^{140}\text{Sm}$  projectiles. The 531 keV transition  $2_1^+ \rightarrow 0_1^+$  de-exciting the first excited state in  $^{140}\text{Sm}$  is clearly visible as well as the 715 keV transition  $4_1^+ \rightarrow 2_1^+$  and the 460 keV gamma-ray, which is related to the decay of the tentatively assigned  $(0_2^+)$  state at 990 keV. The broad structure is related to the excitation of the  $2_1^+$  state in  $^{94}\text{Mo}$ , which is used for normalization.

The analysis of the experimental yields is performed with the coupled-channel Coulomb excitation least-squares search codes Gosia and Gosia2 [1]. Preliminary results suggest that  $B(E2)$  values for transitions between all observed states and the spectroscopic quadrupole moment for the first  $2^+$  state can be extracted.

A complementary measurement of the lifetimes of low-lying excited states in  $^{140}\text{Sm}$  was performed in June 2013 at the Heavy Ion Laboratory, University of Warsaw, Poland, using the recoil-distance Doppler shift technique with the Bucharest plunger device. The results of the ongoing analysis will provide important spectroscopic data as additional input for the Coulomb excitation analysis, significantly reducing the uncertainties of the electromagnetic matrix elements obtained in the ISOLDE experiment.

To resolve any remaining doubts on the spin-parity assignment for the excited  $(0_2^+)$

state at 990 keV and to search for a possible E0 decay to the ground state, a new experiment using conversion-electron spectroscopy will be performed at HIL Warsaw in May 2014. It is expected that the three complementary experiments combined will yield the complete electromagnetic structure of low-lying states in  $^{140}\text{Sm}$ .

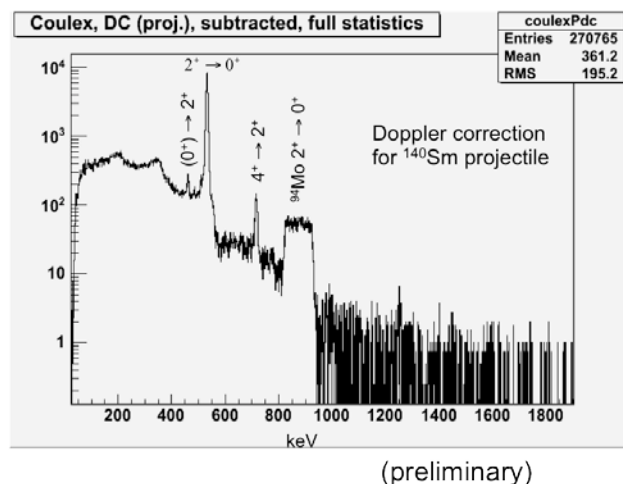


**Fig.1:** Preliminary gamma spectrum from the Coulomb excitation experiment of  $^{140}\text{Sm}$ .

[1] T. Czosnyka, D. Cline, and C.Y. Wu. Bull. Am. Phys. Soc., 28, 745, (1983)

*M.Klintefjord and K. Hadynska-Klek (for IS495 Collaboration)*

## IS496: Evolution of quadrupole collectivity in the N=80 isotones

In the last two newsletters we have reported on the first measurements of the  $B(E2; 2_1^- \rightarrow 0_1^-)$  strength in the radioactive nuclei  $^{140}\text{Nd}$  (2012) and  $^{142}\text{Sm}$  (2013) at the MINIBALL setup. Meanwhile the results have been published [1] or are in preparation [2]. This allows for an overview on the IS496 campaign:

Both isotopes were produced using the RILIS ion source and newly developed ionization schemes for Nd and Sm. In each case Coulomb excitation runs at 2.85 MeV/u were conducted on two different targets. From the  $\gamma$ -ray spectra, collected with MINIBALL, the intensities of the  $2_1^+ \rightarrow 0_1^+$  transitions in projectile and target nuclei could be determined. With the help of the Coulomb excitation code GOSIA2 [3] the  $B(E2)$  values of the projectiles were deduced.

The results are illustrated in comparison with the systematics of the  $N=80$  isotones in Fig. 1. The general trend of growing  $B(E2; 2_1^+ \rightarrow 0_1^+)$  strength moving away from the  $Z=50$  shell closure is expected due to the increase in collectivity when adding more and more valence protons and reproduced by the calculations of two microscopic models (QPM and LSSM, see Ref. [1] for details). However, both calculations describe a smoother increase than what the data suggest. In fact, the E2 transition is suppressed to some extent in  $^{138}\text{Ce}$  and enhanced in  $^{140}\text{Nd}$ . That can be ascribed to the filling of the  $\pi(g_{7/2})$  subshell for  $Z=58$ . The theoretical models do not reproduce this shell effect. In a simplified picture the experimental data can be interpreted as a convolution of two extreme scenarios, a near-linear scaling with valence-proton number (valence correlation scheme) and an extreme shell model scenario, see Fig. 1 and Ref. [1].

It was found earlier that the properties of collective states may be more strongly influenced by the underlying subshell structure than previously thought [4] when mixed-symmetric states (MSSs) were investigated in the  $N=80$  chain. To complete this picture it is necessary to measure the fragmentation of the MSSs of  $^{140}\text{Nd}$  and  $^{142}\text{Sm}$ , which will finally become possible at HIE-ISOLDE (Code IS546).

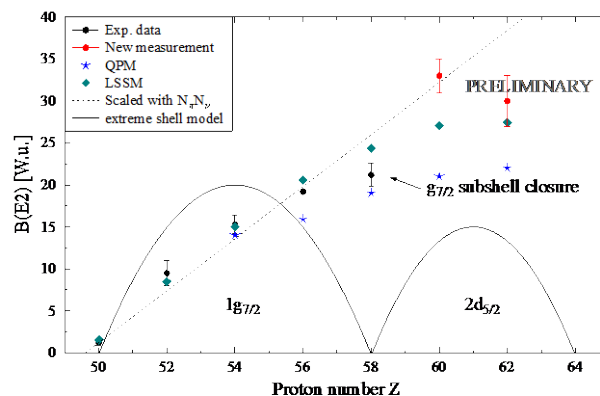


**Fig.1:**  $B(E2)$  in the systematics of the even  $N=80$  isotones from  $Z=50$  ( $\text{Sn}$ ) to  $Z=64$  ( $\text{Gd}$ ). The existing experimental data including our values for  $^{140}\text{Nd}$  [1] and  $^{142}\text{Sm}$  [2] are presented in comparison with theoretical calculations.

The IS496 experiments and their scientific outcome have been the main building blocks for the PhD thesis "Level lifetimes and quadrupole moments from projectile Coulomb excitation of  $A \approx 130$  nuclei" by Christopher Bauer (June 2013).

- [1] C. Bauer et al., Phys. Rev. C 88, 021302(R) (2008)
- [2] R. Stegmann et al., to be submitted to Phys. Rev. C
- [3] T. Czosnyka et al., Bull. Am. Phys. Soc. 28, 745 (1983)
- [4] G. Rainovski, et al. Phys. Rev. Lett. 96, 122501 (2006)

*Christopher Bauer*  
(for the IS496 Collaboration)

## IS506: Coulomb excitation of $^{206}\text{Po}$ and $^{208,210}\text{Rn}$

Nuclei in the vicinity of the  $Z=82$  and  $N=126$  shell closures exhibit features of both single-particle and collective structures in their level patterns. When moving away from the closed shells transition from single-particle regime to collectivity is expected. So

far, however, the transition probabilities to the first  $2^+$  states in neutron-deficient trans-Pb nuclei are mainly unknown. This is mainly due to the seniority  $8^+$  isomers residing on the yrast line and hampering the measurements of state lifetimes. These measurements are unique to ISOLDE as post-accelerated radioactive beams can be studied via Coulomb excitation at MINIBALL.

In the present experiment matrix elements have been measured for the transition to the first  $2^+$  states in  $^{206}\text{Po}$  and  $^{208,210}\text{Rn}$  [1]. The RILIS laser ion source was used to ionise the  $^{206}\text{Po}$  atoms, which were then mass selected by HRS. Due to the long half-life of  $^{206}\text{Po}$  (8.8 d), ISOLDE delivered sufficient yield offline from a  $\text{UC}_x$  target, after its irradiation with protons. Radon as a noble gas was ionised with the VADIS ion source. REX delivered  $^{206}\text{Po}$  (2.85 MeV/u) and  $^{208,210}\text{Rn}$  (2.82 MeV/u) beams to the target position of MINIBALL, where they were Coulomb excited using the secondary 2 mg/cm<sup>2</sup> thick  $^{104}\text{Pd}$  and  $^{116}\text{Cd}$  targets, respectively. The standard Coulomb excitation set-up with a CD detector was used [2]. In Fig. 1 Doppler corrected  $\gamma$ -ray energy spectrum following Coulomb excitation of  $^{208}\text{Rn}$  is shown.

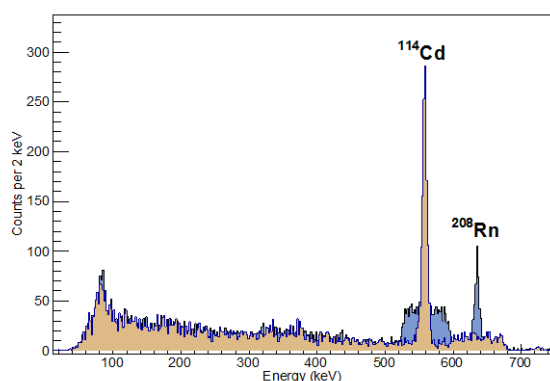


**Fig.1:** Doppler-corrected, background subtracted  $\gamma$ -ray energy spectrum recorded in coincidence with a target-nucleus event in the CD detector. Doppler correction is applied for projectile ( $^{208}\text{Rn}$ , blue) and target ( $^{114}\text{Cd}$ , brown) excitations.

The Coulomb excitation  $\gamma$ -ray yields recorded with MINIBALL were analysed with Gosia2 code, which in favourable cases produced both the transitional and diagonal matrix elements for the first  $2^+$  states. Fig.2 shows preliminary results obtained for  $^{208}\text{Rn}$ , in which simultaneous minimisation has been carried out for both the target and projectile  $\gamma$ -ray yields. The full results will be published later.

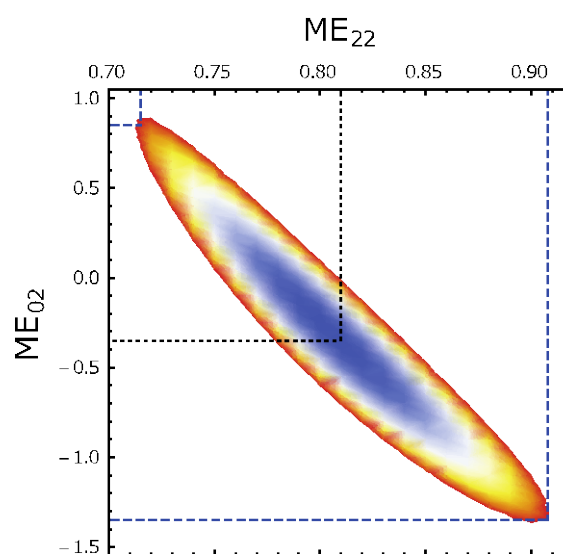


**Fig.2:** Sum of  $\chi^2$  values resulting from Gosia2 minimisation as a function of the diagonal ( $ME_{22}$ ) and transitional ( $ME_{02}$ ) matrix elements (in eb) for the first  $2^+$  state in  $^{208}\text{Rn}$ .

[1] T. Grahn et al., EPJ web of conferences 63, 01009 (2013).

[2] N. Warr et al., Eur. Phys. J. A 49, 40 (2013).

*Tuomas Grahn for the IS506 Collaboration*

## IS530: Beta decay of $^{34}\text{Mg}$

More than three decades after the first clues [1, 2] to the existence of a region of deformation and/or shape coexistence around  $N=20$  - the so-called "Island of Inversion" - one can still find nuclei in its vicinity for which the experimental information is scarce. Such an example is

the heaviest nucleus inside this 'island' –  $^{34}\text{Mg}$ , whose first beta-gamma spectroscopy was performed recently at ISOLDE [3]. The daughter nucleus –  $^{34}\text{Al}$  – had no experimental level scheme, though some transitions were previously assigned to this nucleus [4, 5]. Moreover a low spin beta-isomer of unknown excitation energy was evidenced at GANIL [6], presumably the  $1^+$  state build on  $1\hbar\omega$  configuration [3,7], populating strongly the deformed  $O_2^+$  isomer in  $^{34}\text{Si}$  of intruder origin.

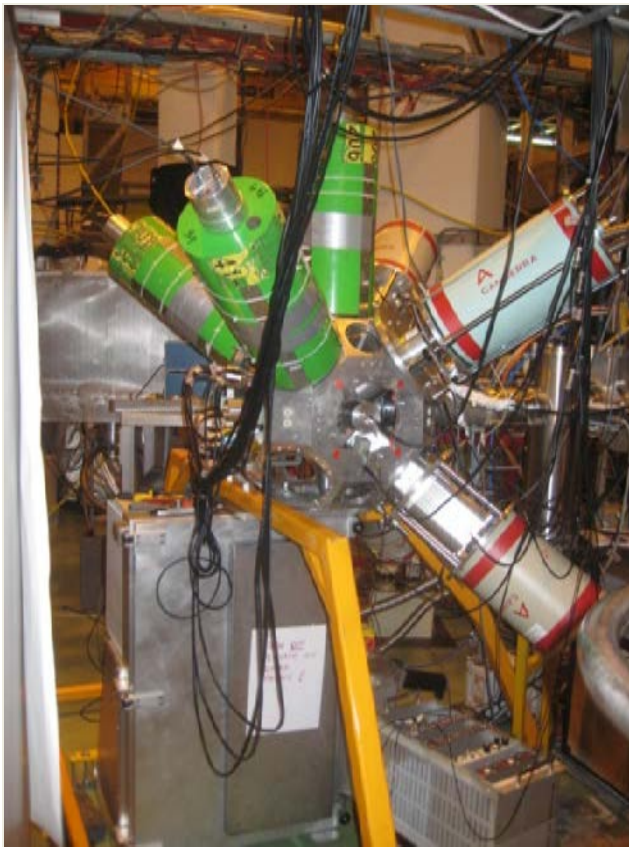


**Fig.1:** The IS530 detection array.

The detection array shown in Figure 1 can be viewed as a prototype of the ISOLDE Decay Station under construction and consisted of the OSIRIS mechanical frame, HPGe detectors (3 Clovers + 1 Coaxial), 5  $\text{LaBr}_3(\text{Ce})$  detectors, 3 neutron detectors

(NE213 liquid scintillator) and a beta detector (NE102 plastic scintillator).

The gamma spectrum following the beta-decay of  $^{34}\text{Mg}$  and gamma coincidence analysis led to the preliminary  $^{34}\text{Al}$  level scheme built on top of the -presumably-  $1^+$  isomer, displayed in Figure 2.

It is worth mentioning that all of the 22 gamma transitions in  $^{34}\text{Al}$  reported in this experiment are observed for the first time

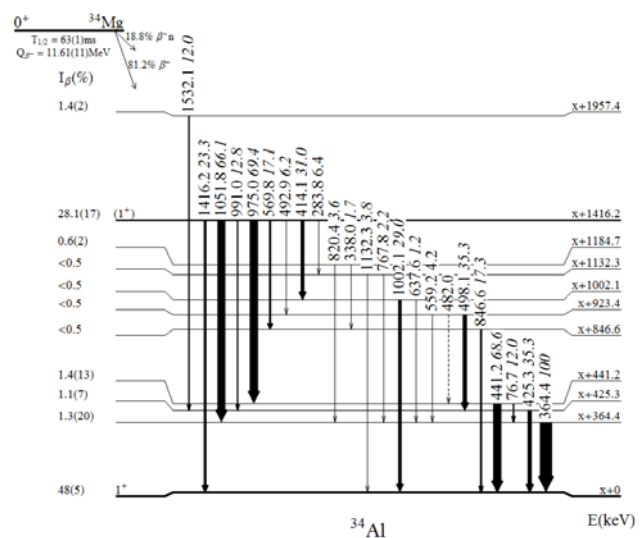


**Fig.2:** Preliminary beta-decay scheme of  $^{34}\text{Mg}$  (level energies in  $^{34}\text{Al}$  are relative to the  $1^+$  isomeric state of unknown excitation energy)

[4, 5]. The delayed gamma transition  $1^+ \rightarrow 4^-$  was not observed, most likely as a result of a small excitation energy of the isomer. Also, none of the observed gammas in prompt coincidence with a beta trigger could be connected to the  $4^-$  state of  $^{34}\text{Al}$ . Therefore, none of the available information can help to decide which of the  $4^-$  and  $1^+$  states is the ground state of  $^{34}\text{Al}$ . For all these reasons, a mass measurement with ISOLTRAP was proposed and accepted [8]. The beta-decay half-life of  $^{34}\text{Mg}$  was determined using the beta-gated gamma time with respect to the proton pulse leading to  $T_{1/2} = 63(1)$  ms, three times larger than the previously measured value determined from beta-neutron coincidences

[9]. This new value is also confirmed by the beta-gated time spectra using known gamma transitions in  $^{33}\text{Al}$  (populated in the beta-n decay of  $^{34}\text{Mg}$ ).

The subsequent beta-decay of the  $1^+$  in  $^{34}\text{Al}$  revealed several new gamma transitions in  $^{34}\text{Si}$ . The absence of gammas (such as 124 keV) that were previously shown to be fed in the beta-decay of the  $^{34}\text{Al}$   $4^-$  ground state [10], is the proof that the  $4^-$  state is not populated in the beta-decay of  $^{34}\text{Mg}$  (not even indirectly despite the large number of excited states found in  $^{34}\text{Al}$  that could have a small gamma branch to the  $4^-$  state).

To conclude, the gamma transitions following the beta decay of  $^{34}\text{Mg}$  have been observed for the first time. All the transitions fed a presumably  $1^+$  state.

- [1] C.Thibault et al., PRC 12, 644 (1975)
- [2] C.Detraz et al., PRC 19, 164 (1979)
- [3] F. Negoita et al., INTC-P-314 (2011)
- [4] M.Gelin, PhD thesis, Univ. de Caen (2007)
- [5] B.V.Pritychenko et al., PRC 63, 047308 (2001)
- [6] F.Rotaru et al., PRL 109, 092503 (2012)
- [7] P.Himpe et al., PLB 658, 203 (2008)
- [8] P.Ascher et al., INTC-P-372 (2013)
- [9] M.Langevin et al., Nucl. Phys. A 414, 151 (1984)
- [10] S.Numella et al., PRC 63, 044316 (2001)

*R.Lica, F. Negoita, S. Grevy and F. Rotaru  
(for the IS530 Collaboration)*

## IS532: Multi-reflection time-of-flight mass spectrometry reveals $N = 32$ shell effect

The challenging quest for measuring the ground state properties of very exotic isotopes requires the application of new techniques that allow coping with highly contaminated primary beams in which only

a few of the short-lived ions of interest are present. The introduction of a multi-reflection time-of-flight mass spectrometer (MR-ToF MS, see Fig. 1) as part of the precision mass spectrometer ISOLTRAP at ISOLDE/CERN, opened the door for measurements under such extreme conditions [1].

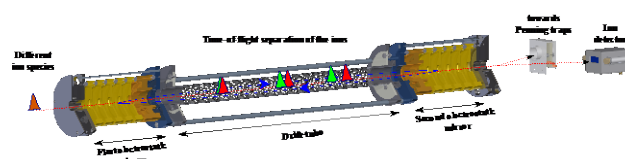


*Fig. 1: Sketch of the MR-ToF MS at ISOLTRAP*

The 2012 mass measurements of the neutron-rich calcium isotopes up to  $N = 34$  within the IS532 experiment have demonstrated this capability.

For  $A = 51$  and 52, the well-established Penning-trap ToF-ICR technique was applied, where the MR-ToF MS was used to supply the traps with purified calcium ion bunches. For the less abundant calcium isotopes  $^{53}, ^{54}\text{Ca}$ , the MR-ToF device itself was employed to measure the masses of the ions via their respective flight times [2]. Chromium isobars from ISOLDE were used as reference ions for the time-of-flight calibration.

In Fig.2 the empirical two-neutron shell gap,  $D_{2n} = 2B(Z, N) - B(Z, N-2) - B(Z, N+2)$ , with  $B$  the nuclear binding energy, is plotted as a colour-coded nuclear chart. The enhancement of  $D_{2n}$  marking the magic neutron numbers  $N=20$  and  $N=28$  is visible, together with the  $N=Z$  enhancement known as the Wigner effect. With the new mass values one also finds a large  $D_{2n}$  for  $N=32$  in the calcium isotopic chain ( $Z=20$ ), which establishes its magicity in that region of the nuclear chart.

The new mass values challenge state-of-the-art theoretical models, presented in Fig. 3. Shell-model calculations based on chiral-effective-field theory including three-

nucleon forces (NN+3N), performed by physicists at the TU Darmstadt [3],

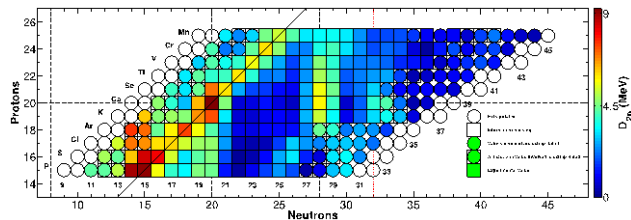


**Fig.2:** Chart of nuclides around  $Z=20$ , where the colors correspond to the empirical two-neutron shell-gap values.

reproduce the data even better than calculations with phenomenological interactions (KB3G, GXPF1A) [4, 5]. The former are only constrained to nucleon-nucleon scattering data and to the properties of very light nuclei. This excellent agreement is encouraging in the long-term attempt to establish a link between nuclear-structure observables and the fundamental theory of quarks and gluons and to provide reliable predictions for the nuclei even farther from stability.

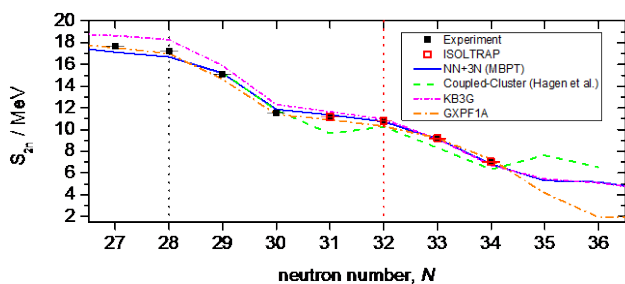


**Fig.3:** Two-neutron separation energy as a function of the neutron number for neutron-rich calcium isotopes.

[1] R.N. Wolf *et al.*, Int. J. Mass Spectrom. 349-350, 123 (2013).  
 [2] F. Wienholtz *et al.*, Nature 498, 346 (2013).  
 [3] J. D. Holt, J. Menendez and A. Schwenk, J. Phys. G- Nucl. Part. Phys. 40 (2013) 075105.  
 [4] A. Poves *et al.*, Nucl.Phys. A 694, 157 (2001).  
 [5] M. Honma *et al.*, Eur. Phys. J. A 25, s01, 499 (2005).

*Frank Wienholtz (for the ISOLTRAP Collaboration)*

## IS535: An unexpected journey to explore the nuclear shapes of rubidium and caesium isotopes

At the end of the 2012 ISOLDE experimental campaign, the masses of several neutron-rich rubidium (Rb) and caesium (Cs) isotopes were determined with the mass spectrometer ISOLTRAP. Initially, mass measurements of neutron-rich copper (Cu) isotopes had been scheduled, but those had to be cancelled due to unexpected difficulties with the target unit. However, the target provided enough surface ionized beams for an alternative program. As a result, precision mass measurements of  $^{98-100}\text{Rb}$  and  $^{132,144-148}\text{Cs}$  isotopes were performed. All mass values have been improved significantly and even the mass of  $^{100}\text{Rb}$  was measured for the first time. Furthermore, with a half-life of 51(8) ms [1], this nuclide is the shortest-lived ever measured at ISOLTRAP.

Of particular importance for nuclear theory are the nuclei found in transitional regions between spherical and deformed shapes. The neutron-rich, mid-shell isotopes of Rb and Cs belong to these species. The isotope  $^{100}\text{Rb}$  is located in the well-known  $A \sim 100$  shape-transition region, while the isotope  $^{148}\text{Cs}$  is located in a region where sudden nuclear-shape transitions are expected due to corresponding changes in the configuration of the nuclear ground states. These are visible as kinks in the two-neutron separation energy ( $S_{2N}$ ) as a function of the neutron number  $N$ . Our experimental values, in the case of  $^{148}\text{Cs}$ , show an increase in the binding energy supporting the hypothesis for complex nuclear shape of its ground state.

In the upper part of Fig.1 the experimental  $S_{2N}$  values of Rb [2-4] and Kr isotopes [4-5] are presented. A previous ISOLTRAP experiment showed that in the Kr chain  $S_{2N}$  is linearly decreasing [5], leading to the

conclusion of there being no sudden shape transition up to  $N = 61$ . In contrast to Kr, the isotopic chain of Rb, now including the new mass values [6], clearly shows the transition to a different stable configuration at  $N = 60$ .

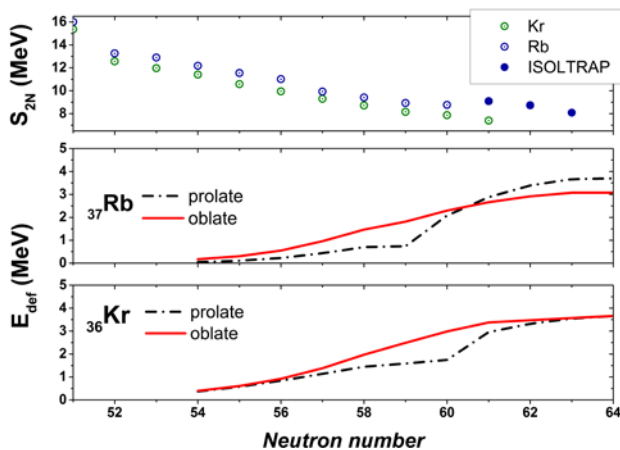


**Fig. 1:** Two-neutron separation energy ( $S_{2N}$ ) for isotopes of Kr and Rb (upper panel) and deformation energy ( $E_{\text{def}}$ ) of the prolate and oblate configurations along the two isotopic chains (middle and lower panel).

To study the origin of this behaviour, we have performed Hartree-Fock-Bogoliubov calculations using the HFODD code [7] and the SLy4 interaction [8]. Each nucleus has two equilibrium shapes (oblate and prolate, respectively). The 2<sup>nd</sup> and 3<sup>rd</sup> panels of Fig.1 compare the binding energies of the two equilibrium configurations for Rb and Kr by showing the so-called deformation energy,  $E_{\text{def}}$ , where the energy of the spherical solution has been subtracted to facilitate comparison. The configuration with higher binding energy is interpreted as the ground-state.

For the Rb isotopic chain, the calculations show that at  $N=60$  the prolate configuration undergoes a sudden change of deformation energy and also becomes more bound than the oblate, leading to the increase in the  $S_{2N}$  trend. In the case of Kr, the change of

prolate deformation energy takes place at higher neutron number and does not change the ordering between the two configurations. A persistence of the oblate configuration or transition to prolate at higher neutron number are possible explanations for the linear  $S_{2N}$  of Kr isotopes trend up to  $N = 61$ .

- [1] B. Singh, NDS-A=100, 109, 297-516 (2008)
- [2] V. V. Simon, *et al.* PRC 85, 064308 (2012)
- [3] G. Audi, *et al.* Nucl. Phys. A 449, 491 (1986)
- [4] M. Wang, *et al.* Chinese Phys. C 36, 1603 (2012)
- [5] S. Naimi *et al.* PRL 105 032502 (2010)
- [6] V. Manea *et al.* PRC 88 054322 (2013)
- [7] N. Schunck, *et al.* Comp. Phys. Commun. 183, 166 (2012)
- [8] E. Chabanat, *et al.* Nucl. Phys. A 635, 231 (1998)

*Dinko Atanasov (for the ISOLTRAP Collaboration)*

## Target and Ion Source Development (TISD):

For this past year, the target and ion source development activities have been adapted to the specificities of LS1 (Long Shutdown 1). The focus was therefore shifted to the design of new target materials and ion sources using the infrastructures available at CERN, and tests done outside within different collaborative frameworks. In the following article we provide some details of molten targets developments, which besides observed or expected improvements of some of the beams at ISOLDE, have potential applications for high power facilities and for hadron therapy. The production of molecular beams of  $^{44}\text{Ti}$  and of exotic Boron ions exploiting an intense neutron source is ongoing and developments are reported here. We conclude this report with news on post-irradiation investigations carried out for the first time on  $\text{UC}_x$  targets.

Research and development work in molten targets has been split between two different types of materials: molten salts and molten metals. The molten salt ( $\text{NaF}:\text{LiF}$ ) target on-line tests, carried out in 2012, yielded promising results [1]. In particular, record intensities of  $^{11}\text{C}$  ( $8 \times 10^8$   $^{11}\text{CO}/\mu\text{C}$ ) have been measured, showing an improvement by two orders of magnitude in comparison with the best figures reported in the ISOLDE database. These intensities are relevant in the production of radiotracers for nuclear imaging. In fact, by using a more suitable proton beam driver (e.g. 30 MeV, 1.2 mA typical for commercial cyclotrons) and accounting for the extraction and post-acceleration efficiencies, the production of intense  $^{11}\text{C}$  beams using ISOL molten salt targets could be used to perform hadron therapy and treatment dose distribution mapping at the same time. Additional

studies will be needed to validate the technical feasibility of this approach.

A new project involving molten targets has been initiated in 2012, defined under the acronym LIEBE (Liquid Eutectic Pb Bi target loop for EURISOL). A target unit is in the process of being prototyped to improve the intensities of short-lived mercury and astatine isotopes. It is inspired by the lead bismuth eutectic (LBE) target loop, which was proposed by E. Noah et al., and tested offline during EURISOL-DS [2]. As an important step for the validation of the concept, the LBE loop compatible with the Isolde robot handling and Front-ends is now in the design phase (Fig. 1). The molten LBE will be irradiated in a dedicated volume, then will pass a metallic grid where a shower will be created, facilitating the diffusion of the produced isotopes and, thus, increasing the released fraction of short-lived nuclides. The molten metal will be kept circulating with an electromagnetic pump.

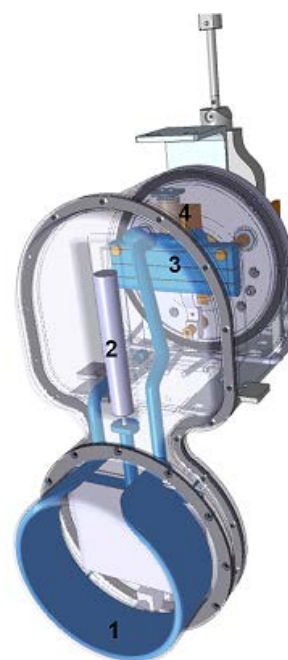


*Fig. 1: Layout of the LIEBE target: 1. electromagnetic pump, 2. dump tank, 3. irradiation and diffusion chambers, and 4. condensation chimney and transfer line.*

Primary focus is given to the dimensioning of the diffusion chamber, where the LBE shower will be formed, leading to expected release fractions for exotic Hg isotopes such as  $^{177-178}\text{Hg}$  [3].



**Fig. 2:** LBE shower at the exit of the metallic grid.

The first offline tests to investigate the feasibility of the shower formation have been performed using a metallic grid with 100  $\mu\text{m}$  radius pores spaced by 300  $\mu\text{m}$ . Fig. 2 shows a picture of the first LBE shower obtained at ISOLDE. Additional offline tests to commission the prototype are foreseen this year before the on-line run expected in 2015.

Beams of short lived isotopes of light elements such as  $^9\text{C}$ ,  $^{17}\text{C}$  and  $^8\text{B}$  are desired for a variety of experiments [4,5]. However efficient extraction of short lived isotopes from target units is difficult due to several reasons. Both elements have a very high boiling point (2550 $^\circ\text{C}$  for B & 3520 $^\circ\text{C}$  for C) and are chemically reactive at the operating temperatures of the ISOLDE target units. By the choice of target material or injection of specific gases the formation of more volatile molecules such as boron fluorides or carbon oxides can be promoted. This approach was used to extract  $^{44}\text{Ti}$  as  $^{44}\text{TiF}_3^+$  during the IS543 run in 2012 [6]. The high chemical reactivity of boron and carbon eases the formation of molecules necessary for extraction. However it is also responsible for losses during extraction.

The design of ISOLDE targets requires the use of refractory metals such as tantalum, rhenium and molybdenum. Calculations of the chemical equilibria of boron and carbon with these metals show that the formation of borides and carbides is favoured over the formation of fluorides and oxides. Therefore each material has to be considered separately, chosen carefully and if possible substituted.

A first step in the extraction of isotopes from target units is the diffusion of the isotopes to the surface of the target material where it can form a molecule. While the diffusion of carbon in target materials has extensively been studied [7], few investigations focused on the diffusion of boron [8]. To further investigate this,  $^{10}\text{BF}_2^+$  is implanted into target samples at the offline mass separator combined with a standard target unit. This is done by reacting elementary boron in the production unit with injected  $\text{SF}_6$  to form volatile  $\text{BF}_2$ .

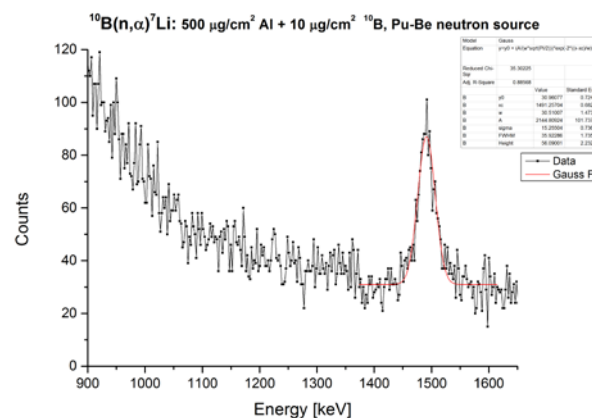


**Fig. 3:** Spectrum of the  $^{10}\text{B}(n,\alpha)^7\text{Li}$  reaction. The investigated sample is used to calibrate the measurement.

After implantation, the samples are exposed to a thermal neutron field while positioned in front of an alpha detector. The high neutron capture cross section of  $^{10}\text{B}$  of  $\sigma=3840$  b allows the distribution of boron in the sample to be determined by detecting alpha particles from the  $^{10}\text{B}(n,\alpha)^7\text{Li}$  reaction.

Fig. 3 shows a typical spectrum from such a measurement. After determining the initial distribution the samples are heated to temperatures up to 1000°C in order to promote diffusion. Repeating the irradiation allows diffusion properties of boron in the material to be characterised. These measurements will help to choose a target material with the best diffusion properties, allowing the improvement of the extraction of B beams.

After more than 40 years,  $UC_x$  is still a reference material for ISOL-type isotope production. In the ENSAR-FP7 JRA ACTILAB this material, its isotope release properties and de-novo designed enhanced matrices are under investigation. A combined suite of advanced synchrotron-based techniques has been developed [9] to characterize the uranium mixed carbide material that is currently used at ISOLDE. These experiments have been performed at the Swiss Light Source (SLS) during several beam times, yielding novel findings that might explain this material's outstanding stability during operation at high temperature and high-energy proton irradiation on the sub-microscopic level [10]. In order to follow and understand the performance evolution of a target material, post-irradiation studies are indispensable, preferably from a target unit where release properties were closely followed online. Therefore, for the first time in history, an irradiated uranium carbide target has been dismantled and the material extracted for further analysis. The ISOLDE production unit #466 that had been used twice for isotope production in 2011 was sent to PSI, where it was dismantled in a special chain of hot cells. Finally the material was extracted and tiny subsamples of only a few  $\mu\text{m}^3$  were prepared using a nano-focused Gallium ion beam [11], allowing their radioactivity to decrease sufficiently to

study them in a class C environment at the microXAS beamline (SLS).

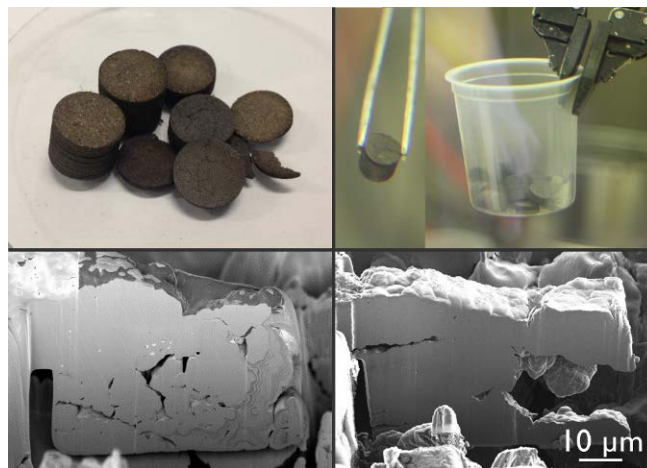


*Fig. 4: ISOLDE  $UC_x$  before (left) and after (right) proton irradiation at ISOLDE. The  $\varnothing 14$  mm material pellets (top) are subject to very little change, while the microscopic structure (bottom) evolved considerably.*

Fig. 4 shows images of conventional ISOLDE  $UC_x$  before and after irradiation. While the macroscopic appearance has hardly changed due to the harsh conditions during operation, the microscopic structure has been subject to sintering and complex phase transformations [10,12]. These results have been translated into the synthesis of new uranium mixed carbide materials, one of which was tested online at ISOLDE in December 2012 with promising results [13]. Further experiments are planned in 2014, both at ALTO-IPNO and at ISOLDE.

[1] T.M. Mendonca et al., CERN-ACC-NOTE-2013-0009 (2013).

[2] Final Report of the EURISOL Design Study, J. Cornell Ed., Ganil, 2009.

[3] L.C. Carraz, et al., Nucl. Instr. Meth. 158 (1979) 69.

[4] A. DI Pietro et al., CERN-INTC-2010-063; INTC-I-126.

[5] H. Fynbo et al., CERN-INTC-2006-011; INTC-P-207.

- [6] V. Margerin et al., submitted to Phys. Lett. B.
- [7] H. Franberg, CERN-THESIS-2008-084.
- [8] J. Vacik et al., AIPC, Twentieth International Conference. AIP Conference Proceedings, Volume 1099, pp. 836-839 (2009).
- [9] A. Gottberg et al., ISOLDE Newsletter 2013 (2013).
- [10] A. Gottberg et al., submitted.
- [11] C. Degueldre, et al., Talenta, 106, 408-413 (2013).
- [12] A. Gottberg et al., in preparation.
- [13] T. Stora, Nucl. Instr. Meth. Part B, 317, 402-410 (2013).

*T.M. Mendonca, C. Seiffert, A. Gottberg*

## How to obtain access to the ISOLDE hall

1. Register at the CERN Users office<sup>1</sup> (Opening hours: 08:30 - 12:30 and 14:00 – 16:00 but closed Wednesday mornings). You need to bring
    - a. [Registration form](#) signed by your team leader or deputy<sup>2</sup>
    - b. [Home Institution Declaration](#)<sup>3</sup> signed by your institute's administration (HR).
    - c. Passport
  2. Get your CERN access card in [Building 55](#)
- With this registration procedure you become a **CERN user**<sup>4</sup>.
3. Follow the CERN basic safety course (levels 1 to 3):
    - a. If you have a CERN account, you can access the Safety Awareness course on-line at the web page <http://sir.cern.ch>, from your computer, inside or outside CERN.
    - b. If you have not activated your CERN account, there are some computers available for use without the need to log in on the first floor of building 55 (Your CERN badge will be needed in order to prove your identity).
  4. **Until July 1<sup>st</sup> 2014:**  
Follow the online [RP course for Supervised Radiation](#). If you have not activated your CERN account see 3b.  
**After July 1<sup>st</sup> 2014:**  
Follow the ISOLDE online RP Course. If

you have not activated your CERN account see 3b.

5. Obtain a Permanent radiation dosimeter at the Dosimetry service, located in [Building 55](#)<sup>5</sup> (Opening hours: Mon. to Fri. 08:30 – 12:00). The dosimeter should be returned to the Dosimetry service at the end of your visit.  
**Until July 1<sup>st</sup> 2014:**  
A [medical certificate](#)<sup>6</sup>, valid for 24 months, is required.  
**After July 1<sup>st</sup> 2014:**  
The RP form (presently under preparation) signed by your institute will be required. You will also have to follow a 2 hour practical RP safety course for which you will have to register in advance.
6. Apply for access to "ISOHALL" using EDH:  
<https://edh.cern.ch/Document/ACRO>. This can be done by any member of your collaboration (typically the contact person) having an EDH account<sup>7</sup>. Until July 1<sup>st</sup> 2014 access is recorded in your card, after July 1<sup>st</sup> it will be recorded in your dosimeter.

Find more details about CERN User registration see the [Users Office website](#). For the latest updates on how to access the ISOLDE Hall see the [ISOLDE website](#).

New users are also requested to visit the ISOLDE User Support office while at CERN.  
Opening hours:  
Mon., Tues., Thurs., Fri. 08:30-12:30  
Mon. & Thurs. 13:30-15:30

<sup>1</sup> <http://cern.ch/ph-dep-UsersOffice> (Building 61, open 8:30-12:30 and 14:00-16:00, closed Wednesday morning).

<sup>2</sup> Make sure that the registration form is signed by your team leader before coming to CERN or that it can be signed by the team leader or deputy upon arrival.

<sup>3</sup> The Home Institute Declaration should not be signed by the person nominated as your team leader.

<sup>4</sup> The first registration as USER needs to be done personally, so please note the opening hours. If needed the extension of the registration can be delegated or performed on-line via EDH.

<sup>5</sup> <http://cern.ch/service-rp-dosimetry> (open only in the mornings 08:30 - 12:00).

<sup>6</sup> The medical certificate must be brought in person to the Dosimetry Service (either by the user or a representative)

<sup>7</sup> Eventually you can contact Jenny or the Physics coordinator.

## Contact information

### ISOLDE User Support

Jenny Weterings

[Jennifer.Weterings@cern.ch](mailto:Jennifer.Weterings@cern.ch)

+41 22 767 5828

### Chair of the ISCC

Yorick Blumenfeld

[yorick@ipno.in2p3.fr](mailto:yorick@ipno.in2p3.fr)

+33 1 69 15 45 17

### Chair of the INTC

Klaus Blaum

[Klaus.Blaum@mpi-hd.mpg.de](mailto:Klaus.Blaum@mpi-hd.mpg.de)

+49 6221 516 851

### ISOLDE Physics Section Leader

Maria J.G. Borge

[mgb@cern.ch](mailto:mgb@cern.ch)

+41 22 767 5825

### ISOLDE Physics Coordinator

Magdalena Kowalska

[Magdalena.Kowalska@cern.ch](mailto:Magdalena.Kowalska@cern.ch)

+41 22 767 3809

### ISOLDE Technical Coordinator

Richard Catherall

[Richard.Catherall@cern.ch](mailto:Richard.Catherall@cern.ch)

+41 22 767 1741

### HIE-ISOLDE Project Leader

Yacine Kadi

[Yacine.Kadi@cern.ch](mailto:Yacine.Kadi@cern.ch)

+41 22 767 9569

More contact information at

[http://isolde.web.cern.ch/contacts/](http://isolde.web.cern.ch/contacts/isolde-contacts)

[isolde-contacts](http://isolde.web.cern.ch/contacts/isolde-contacts) and at

[http://isolde.web.cern.ch/contacts/](http://isolde.web.cern.ch/contacts/people)

[people](http://isolde.web.cern.ch/contacts/people)